UC Irvine
UC Irvine Electronic Theses and Dissertations

Title

A multifaceted exploration of hydrologic drought using GRACE satellite observations and computer modeling

Permalink

https://escholarship.org/uc/item/4wh500mf

Author

Thomas, Alys Caitlyn

Publication Date

2014

Peer reviewed|Thesis/dissertation

UNIVERSITY OF CALIFORNIA,
IRVINE

A multifaceted exploration of hydrologic drought using GRACE satellite observations

and computer modeling

DISSERTATION

submitted in partial satisfaction of the requirements
for the degree of

DOCTOR OF PHILOSOPHY

in Earth System Science

by

Alys Caitlyn Thomas

Dissertation Committee:
Professor James Famiglietti, Chair
Professor Francois Primeau
Professor Jim Randerson

2014

DEDICATION

To the pursuit of knowledge … and happiness

TABLE OF CONTENTS

LIST OF FIGURES

LIST OF TABLES

ACKNOWLEDGEMENTS

I first want to thank my parents for combining their genes to produce me in the first place. The inquisitive, logical, and methodical person I turned out to be has driven and enabled me to complete this graduate school journey. Without the care, discipline, and love from my parents throughout my lifetime, I would not be where I am today and appreciate the sacrifices they often made for me to be in a position where I could excel. Thank you Mom for always reminding me that I can accomplish anything I can dream of in this world and never letting me give up when something was hard to do. Thank you Dad for your love, support, and encouragement, especially when I struggled to find the positive side to life.

Thank you to my sister, Nyssa, for being a rock-solid and down right amazing sibling. You're a role model who is beautiful, driven, and accomplished. Love you. Also thank you to my sister/friend, Jakia, for your friendship, inspiration and staying up until the wee hours of the morning discussing life, love and ambitions. Thank you to my family (aunties, uncles and cousins) and friends who have endured this journey with me and stood by me through this rollercoaster ride.

Thank you to the love of my life, Kelley, for finding a way to make me smile, even when I didn't want to, and bringing tons of joy, unconditional love, and friendship into my life. You are an irreplaceable part of my world and I love you so very much.

Thank you to my Ph.D. adviser, Jay Famiglietti, for accepting me into his research group. You not only supported my work but you taught me the importance of communicating what we do to both government entities and the public sector. Thank you to my committee (Francois, Jim, Jin-Yi, Jasper, and Russ) for all of your comments and advice on focusing and improving my research. I also thank all of the graduate students, post-docs, and researchers that have rotated through Jay's group for their feedback and opinions as I shared half-baked ideas during our group meetings.

Lastly, I want to give a very special thank you to Matt Rodell, Hiroko Beaudoing and Bailing Li at Goddard Space Flight Center, as well as J.T. Reager, Caroline de Linage, Min-Hui Lo, Neeta Bijoor, Brian Thomas, and Cédric David for their mentorship, advice and, most of all, patience.

CURRICULUM VITAE

Alys Caitlyn Thomas

Education

2014	Ph.D. in Earth System Science, University of California Irvine, Irvine, California Advisor: Dr. James Famiglietti, Professor of Earth System Science <u>Dissertation</u>: A multifaceted exploration of hydrologic drought using GRACE satellite observations and computer modeling
2011	M.S. in Earth System Science, University of California Irvine, Irvine, California
2009	M.S. in Soil, Water, and Environmental Science, University of Arizona, Tucson, Arizona Advisor: Dr. Michael Crimmins <u>Thesis</u>: Statistical evaluation of NDVI-climate relationships for drought monitoring in Arizona
2004	B.S. in Environmental Science, Meteorology, Florida Institute of Technology, Melbourne, Florida

Fields of Study

Hydrology and Remote Sensing, Climate Change and Extremes, Soil Science, and Meteorology

Publications

Thomas, A. C., J. T. Reager, J. S. Famiglietti, M. and Rodell (2014). A GRACE-based water storage deficit approach for hydrological drought characterization. *Geophys. Res. Lett.*, 41(5), 1537-1545.

Selected Presentations

Thomas, A., J. T. Reager, J. S. Famiglietti, and M. Rodell (Dec 2013, Feb 2014), GRACE-observed water storage deficits for hydrological drought characterization, *Oral Presentations, American Geophysical Union Fall Meeting,* Session H32F. Remote Sensing Applications for Water Resources Management II. & *94th Annual American Meteorological Society Meeting,* Conference on Hydrology.

Thomas, A., J. T. Reager, and J. S. Famiglietti (Dec 2012, Jan 2013), Statistical characterization of terrestrial water storage variability and drought on multiple scales within GRACE satellite footprints: *Poster, American Geophysical Union Fall Meeting, San Francisco, CA. & Oral Presentation, 93rd Annual American Meteorological Society Meeting*, Conference on Hydrology.

Thomas, A., M. Rodell, and J. S. Famiglietti (2011) Distinguishing Regional Drought Characteristics Using GRACE Terrestrial Water Storage Datasets*: Poster presented at the NASA Global Drought Monitoring Workshop, April 11-12, 2011.*

Awards And Honors

- NASA Graduate Student Research (GSRP) Fellowship: $30,000 Ann. (2010-2013)
- University of Arizona/NASA Space Grant Graduate Fellowship: $24,000Ann. (2008-2009)
- *Ambassador*, 2013 NASA Student Ambassadors Program
- 2nd place student oral presentation, 2013 American Meteorological Society Annual meeting
- 1st place student oral presentation, 2014 American Meteorological Society Annual meeting

Teaching Experience

Department of Earth System Science, University of California, Irvine, 2013
Teaching assistant:
- General Education Science course, *Hurricanes, Tsunamis, and other Catastrophes*
- Upper Division course, *Fundamentals of GIS for Environmental Science*
- General Education Science course, *Physical Geology*
- General Education Science course, *The Atmosphere*

Department of Soil, Water, and Environmental Science, University of Arizona, 2007
Teaching assistant for Lower Division course, *Introduction to Environmental Science*

Organizations

- American Geophysical Union
- American Meteorological Society
- National Ground Water Association
- Orange County Graduate Women in Science (*OCGWIS*)
- Volunteer, Climate, Literacy Empowerment And iNquiry (*CLEAN*) Youth Science Education

ABSTRACT OF THE DISSERTATION

A multifaceted exploration of hydrologic drought using GRACE satellite observations

and computer modeling

By

Alys Caitlyn Thomas

Doctor of Philosophy in Earth System Science

University of California, Irvine, 2014

Professor James Famiglietti, Chair

Prolonged hydrologic drought disturbs the natural state of ecosystems, stresses regional water supplies, and can adversely affect agricultural production. Determining the severity of hydrologic drought traditionally depended on evaluations of historical rainfall, stream flow, and soil moisture; yet, a comprehensive measure of the magnitude of a drought's impact on all components of the terrestrial hydrologic system, including surface, soil, and groundwater storage, remains lacking in standard drought analyses. NASA's Gravity Recovery and Climate Experiment (GRACE) satellite mission fills a gap by providing monthly measures of terrestrial water storage anomalies (TWSA) based on time-variable gravitational fields. This dissertation details an investigation of regional hydrological extremes (*e.g.*, drought and flood) using both satellite remote sensing data and outputs from NASA's Catchment Land Surface Model (CLSM).

The first project presented in this thesis involves discussion of a novel quantitative, GRACE-based framework for measuring the severity of hydrologic drought. GRACE observations are used to quantify drought by calculating the deviation of monthly-average

terrestrial water storage anomalies from the regional climatological reference, where negative deviations represent storage deficits. Each deficit conveys the volume of water that would be required to recover from a drought. Moreover, this finite deficit observation allows for the calculation of a likely time for recovery based on statistical percentiles of storage change distributions, for every month through the end of the event.

The second portion of work evaluates and compares the characteristics of subsurface terrestrial water storage variables from the CLSM, assimilated with GRACE satellite observations (CLSM-DA), for the purposes of: acquiring near-real time analysis, downscaling GRACE's spatial resolution, and vertically disaggregating GRACE column-integrated water storage anomalies. Several zones throughout the United States were selected to quantify differences between hydrologic extremes identified by CLSM-DA and those measured by GRACE. Results establish that CLSM-DA TWSA outputs improved those from CLSM Open-loop runs in all regions with R^2 increases from 5-14%. We also compared CLSM surface soil moisture content with independent surface moisture observations from the AMSR-E satellite to assess improvements after data assimilation. Results established that assimilation produced modest improvements in correlations between CLSM and AMSR-E in all regions.

CLSM-DA hydrologic extremes are comparable to GRACE, however the data-assimilated model continues to struggle with matching the some of the amplitudes of extreme events, in part due to model structure and parameters that do not possess enough information about the hydrologic system to accurately depict changes in TWSA as observed by GRACE. Since CLSM continues to run through the near-present month (April 2014), beyond the current, publically available GRACE month (January 2014), an assessment of the CLSM's performance between assimilation updates is also provided.

The final project details the development of a linear multivariate, multi-frequency regression model to estimate monthly water storage change and extremes before and beyond the currently available GRACE observation period (April 2002-April 2014). The regression model provides coefficients that can then be used with any precipitation and evapotranspiration dataset, to calculate the associated amount of water storage change for our study region, California's Central Valley (*e.g.*, Sacramento, San Joaquin, and Tulare river basins). Model results show that 82% of GRACE's TWSA signal can be explained with a combination of precipitation and evapotranspiration. The June 2014 storage estimate from the regression model revealed that water storage deficits persisted in the Central Valley with a monthly value of -28.8 km^3 (±1.22 km^3).

This work concludes that GRACE satellite data can successfully be utilized for regional scale drought analysis and has implications for improving drought early warning lead times together with drought preparation and management efforts. The storage deficit method demonstrates the added benefits of explicitly recognizing the beginning and end of storage deficit periods and of providing additional information about the effects of meteorological drought on regional water storage. Data assimilation increases the usability of GRACE for near-present monitoring, while implementation of the linear multi-frequency regression model allows for the extension of water storage anomalies.

Chapter 1

Introduction

1.1 Defining Drought

The reality of drought is that it is a regularly occurring, physical phenomenon of the climate system in nearly every location on earth. Drought translates to 'disaster' when this natural event meets the demand placed on water and other natural resources by human-use systems [*Wilhite et al.*, 2007]. Droughts have occurred many times in the past and will continue to occur in the future; yet, because of growing water needs around the world, the adverse consequences of droughts will likely worsen. The effects of drought are pervasive and can be devastating from both economical and ecological perspectives. In the 2003-2013 timespan, there were over 530 occurrences of meteorological and hydrological droughts throughout the world, which affected more than 3.7 million people and created a total of over $61 billion in damages [*EM-DAT*, 2014].

> *"One of the first steps in the investigation of any problem is the*
> *definition of the problem itself; herein lies one of the principal*
> *obstacles to the investigation of droughts, for there is a wide diversity*
> *in the ways in which different fields of study view droughts."*
> [*Yevjevich*, 1967]

The definition of a drought is often subjective and only realized by authorities after being well established for a prolonged period of time. *Wilhite et al.* [2007] stated that hundreds of definitions exist, mainly because drought needs to be defined according to the characteristics of

individual climatic regimes and the specific impact sector to which the definition is being applied.

Numerous authors have published definitions of drought. For instance, in the 1950s, the National Weather Service defined drought as: "a lack of rainfall so great and long continued as to affect injuriously the plant and animal life of a place and to deplete water supplies both for domestic purposes and for the operation of power plants, especially in those regions where rainfall is normally sufficient for such purposes" [*Havens*, 1954]. Palmer [1965] generally defined drought as "a prolonged and abnormal moisture deficiency" - a definition that is still supported by the American Meteorological Society. *Yevjevich* [1967] stated that, while the explanation of droughts is primarily related to the physical interactions of cause and effect, the description of droughts encompasses statistical and deterministic characteristics. *Kallis* [2008] provided a "conceptual definition" of drought, which encompasses different operational perspectives but remains narrow enough to distinguish drought from the concepts of scarcity and aridity: "drought is a temporary lack of water, which is, at least partly, caused by abnormal climate conditions and is damaging to an activity, group, or the environment." It is important to note that drought should not be confused with aridity, which is a permanent feature of a dry or desert climate.

Drought definition is exceedingly important in recognizing specific types of drought occurrences so that governing bodies can declare a drought disaster and provide targeted economic relief. *Dracup et al.* [1980] noted that the nature of the water deficit to be studied (*e.g.*, meteorological, hydrological, or agricultural) would determine the general drought definition. The selected category has implications for the direction of research, methodologies employed, and assessment of impacts. To simplify communication of drought concepts and facilitate

management decision support, drought often is categorized into four general types: 1) meteorological or climatological, 2) agricultural, 3) hydrological, 4) socioeconomic [*Dracup et al.*, 1980; *Wilhite and Glantz*, 1985]. Meteorological or climatological drought is simply defined in terms of the magnitude and duration of a precipitation deficiency. Agricultural drought associates precipitation shortages most immediately with higher evapotranspiration levels and soil moisture deficits. The onset of an agricultural drought may lag that of a meteorological drought, depending on the antecedent moisture in the surface soil layers. Socioeconomic drought focuses on the impacts of any of the previous drought types on society.

The concentration of this dissertation research is hydrological drought. *Linsley et al.* [1975] gives a textbook definition of hydrological drought: "a period during which streamflows are inadequate to supply established uses under a given water management system". If flow for a specified period of time falls below that threshold, then hydrological drought is considered to be in progress. A conceptual definition describes hydrological drought as an extended period of time where a region's water supply is in a deficit; often triggered by lack of precipitation and persisting long after a meteorological drought has ended. Water deficits manifest in surface waters (streamflow levels), soil moisture, and groundwater aquifers and can lead to losses in agricultural and industry production as well as drinking and recreational water reserves.

1.2 Causes of Drought: A Broad Perspective

At its core, the primary cause of drought is the occurrence of below normal precipitation, which lies in meso-to-macro scale atmospheric processes resulting from intra-seasonal to multi-decadal climate variability. Global atmospheric circulation produces average, regional climatology, though its characteristics can vary from one year to another. Hot temperatures, low

relative humidity, and drying winds often add to the impact of the lack of rainfall [*Condra*, 1944]. Stronger variations in any given year cause anomalies in atmospheric and hydrological characteristics [*Tallaksen and Van Lanen*, 2004]. Another important causative factor of droughts is oceanic circulation and dynamics, which have average patterns of current and heat storage that affect the weather and climate [*Panu and Sharma*, 2002]. (*e.g.*, significant climatic variations are known to occur when a warm pool, which is normally present in the western Pacific Ocean, moves eastward towards the coast of Peru, commonly referred to in the literature as El Nino Southern Oscillation (ENSO) [*Zhang et al.*, 19996; *Wallace et al.*, 1998; *Sun and Yu*, 2009].

Regional hydrological drought has been linked to a combination of anomalous atmospheric circulation patterns (causing persistent dry weather), changes in the timing of precipitation, and low antecedent soil moisture, groundwater, or lake storage conditions [*Tallaksen and Van Lanen*, 2004]. Although climate is a primary contributor to hydrological drought, there are other factors (*e.g.*, changes in land use, deforestation, land degradation, construction of dams), which can all affect the hydrological characteristics of a basin. Given the adverse effects of drought, there continues to be a pressing need for further in-depth research on drought characteristics and impacts throughout the world.

1.3 Climate Change, Drought, and Water Resources

Climate change is likely to globally increase the areas affected by droughts. The observed impact of climate-system changes on droughts varies regionally, depending on changes to the drivers of drought such as precipitation and temperature and on regional features of the hydro-climatological system [*American Meteorological Society*, 2014]. "The combined impacts of increased temperature, precipitation, and evapotranspiration will affect snowmelt, runoff, and

soil moisture conditions". Semiarid, coastal, and snow-fed basins are particularly exposed [*IPCC*, 2007; *Kallis*, 2008; *IPCC*, 2013]. *Kallis (2008)* states that droughts are not only about decreases in means, but also about increases in variability. According to the IPCC [2013]: "Changes in the global water cycle in response to the warming over the 21st century will not be uniform. The contrast in precipitation between wet and dry regions and between wet and dry seasons will increase, although there may be regional exceptions." The hydrological cycle accelerates in response to the water-holding capacity of the atmosphere and evaporation increases [*Kallis*, 2008]. This change in hydrological variability leaves regions vulnerable to prolonged periods of wet/dry conditions, increased intervals from wet and dry seasons, or combinations of both.

In addition to the physical changes in climate, human-induced stressors continue to tax regional water resources. Major stresses on water resources include: increased competition for available water, population growth, poor water quality, aging urban infrastructure, water allocations to environmental and recreational resources, and groundwater overdraft [*Tallaksen and Van Lanen*, 2004]. *Georgakakos et al.* [2014] expect summer droughts to intensify almost everywhere in the continental U.S. due to longer periods of dry weather and more extreme heat, which leads to increased moisture loss from plants and earlier soil moisture depletion in basins where snowmelt shifts to earlier in the year. Any additional stress from climate change or increased variability will only intensify the competition for water resources.

1.4 Measuring Drought

According to an information statement from *American Meteorological Society* [2013], characteristics of drought include magnitude, severity, duration, spatial extent, timing, and

impacts. Magnitude is often interchanged with intensity, which describes the amount of deviation from some "normal" condition for a specified point or range in time. *McKee et al.* [1993] state that the specification of a time scale in the definition of drought leads to two of the most important characteristics – frequency and duration. Severity accounts for the combination of a drought's intensity and duration. Each drought is unique, but common features of the most severe droughts that have far-reaching human and ecological impacts include long duration, large moisture deficits, and large areal extent, particularly when these impacts occur during a climatological wet season.

The flow of water through the hydrological system depends on both natural processes and human activities throughout the region or watershed. The key to hydrological analyses is determining relationships between these two regimes and drought events [*Tallaksen et al.*, 1997]. Statistical techniques used in drought analysis range from probabilistic [*Chung and Salas*, 2000; *AghaKouchak*, 2014] and frequency analysis [*Stedinger et al.*, 1993] of hydrologic extremes to complex multivariate probability density functions of drought characteristics (*e.g.*, duration, magnitude, and severity) [*Mishra et al.*, 2009; *Katz et al.*, 2002]. These methods often utilize the concepts of run theory [*Yevjevich*, 1967], discrete autoregressive moving average (DARMA) models [*Jacobs and Lewis*, 1978; *Chang et al.*, 1984], or grouping methods [*Panu and Sharma*, 2002].

Drought indices are also very important for monitoring droughts continuously in time and space; for reviews of common drought indices refer to *Heim* [2002], *Keyantash and Dracup*, [2002], and *Hayes* [2006]. Drought monitoring systems, such as the U.S. Drought Monitor [USDM; *Svoboda et al.*, 2002], are based primarily on the information that drought indices provide [*Dracup*, 1991; *Vicente-Serrano and López-Moreno*, 2005]. Unveiled in August 1999 at

a White House press conference, the USDM bases drought intensity on several key indicators (*e.g.*, the Palmer Drought Index (PDSI), Standardized Precipitation Index (SPI), Keetch-Byram Drought Index (KBDI), modeled soil moisture, 7-Day average streamflow, and precipitation anomalies), numerous supplementary indicators (*e.g.*, drought impacts), and local reports from more than 350 expert observers around the country [*U.S. Drought Monitor, 2014*]. The drought severity classification tables show the ranges of each indicator and dryness level, based on statistical percentiles. The USDM corroborates data from local observations of drought conditions and impacts from around the country to produce weekly maps of short- and long-term drought severity and spatial extent.

Though drought monitors gather and process an immense amount of data, measures of the effects of drought conditions on our water storage reservoirs, especially in the subsurface, are still largely unknown, primarily due to sparse or non-existent observation networks. Satellite remote sensing has emerged as a fundamental tool for observing Earth systems, particularly, regional hydrologic dynamics where *in situ* observations are frequently absent. Advances in computer modeling techniques have enhanced drought monitoring through the process of data assimilation where outputs from computer models are adjusted and often times improved with data observed through satellite remote sensing [*Houborg et al.,* 2012*; Werth et al.,* 2009*; Zaitchik et al.,* 2008]; yet, when considering hydrologic drought and water deficits, the question often remains: how much water is actually absent from the region during these dry periods?

1.5 Drought Research and GRACE Satellites

NASA's Gravity Recovery and Climate Experiment (GRACE) satellites, launched in March 2002, make detailed, time-variant, global measurements of Earth's gravity field. Scientists

use time-variable gravity to study ground water fluctuations, sea ice, sea level rise, deep ocean currents, ocean bottom pressure, and ocean heat flux [*Schmidt et al.*, 2008]. Since no global widespread network of surface or subsurface hydrological observations exists, *Ramillien et al.* [2008] assert that advances in satellite gravimetry for monitoring terrestrial water storage are significant and unique for determining changes in total water storage. For applications pertaining to terrestrial hydrology, fluctuations in earth's gravity field are attributed to non-static features, chiefly the mass movement of water over and within the land surface.

GRACE satellites observe total, column-integrated terrestrial water storage changes on monthly time scales, which help convey vital information about Earth's water reservoirs over land, ice, and oceans [*Tapley et al.*, 2004]. GRACE data are expressed as terrestrial water storage anomalies (TWSA), or deviations of total water storage from their mean over the observation period. Though GRACE has a low spatial (~400-500 km) and temporal (ten days to a month) resolution, it is currently the only remote sensing satellite with the ability to measure changes in water storage above and below the land surface, within an accuracy of ~1.5 cm of equivalent water thickness.

GRACE satellite data have been shown to be appropriate for use in drought quantification and offer information about surface and subsurface water resources that were previous not available, especially at regional scales. Several studies have examined drought using gravity-based measures of water storage variations from the GRACE mission. *Yirdaw et al.* [2008] used GRACE to develop a total storage deficit index for characterization of the 2002/2003 Canadian Prairie droughts. *Leblanc et al.* [2009] used a combination of GRACE, *in situ*, and modeled hydrological data to identify water deficits and the rise of different types of drought within the Murray-Darling Basin in southeastern Australia. They also substantiated a

persistent reduction in groundwater storage six years after the onset of the drought. *Hasegawa et al.* [2008] also studied drought in Australia, focusing on the 2006 episode. *Frappart et al.* [2012] used GRACE time series of water volume variations to analyze surface water storage during the 2005 Amazonian drought. *Li et al.* [2012] and *Houborg et al.* [2012] both utilized GRACE TWSA with land models to evaluate drought conditions for watersheds in the United States and Europe.

1.6 Statement of Research

The goal of this dissertation is to advance hydrologic extremes research, with a strong emphasis on drought identification and characterization. While there are many indicators that describe meteorological, hydrological, and agricultural types of drought, scientists are still challenged with quantifying severity and determining recovery from drought conditions, in addition to describing the spatial behavior of drought and flood events. The spatial coverage of drought and flood is of significant importance in planning measures towards the mitigation of impacts [*Panu and Sharma*, 2002]. *Rodell and Famiglietti* [1999, 2001] and *Reager and Famiglietti* [2009] indicate the presence of normal range of terrestrial water storage variability (a maximum and minimum anomaly value that changes over time). There are, however, periods where the anomaly exceeds this normal range, indicating periods of extremely low or high terrestrial water mass. Such behavior is identified and evaluated in the following chapters.

There are three substantial results of this work, which fulfill the research goals: 1) a quantitative approach for the calculation of the amount of water missing from regional storage systems during dry periods; 2) regional-scale identification of the variations in timing of hydrological drought through the vertical structure of the terrestrial subsurface; and 3) the

9

development of a statistical model that determines a simplified relationship between precipitation amount and subsequent changes in terrestrial water storage.

1.7 Dissertation Outline

Work presented in the following chapters concentrates on the use of modern technologies (*e.g.*, satellite remote sensing and computer modeling) for the improvement of hydrological drought characterization and monitoring efforts. This body of work consists of three projects, organized into three chapters:

Chapter 2: Introduction of a novel approach to characterizing hydrological drought with terrestrial water storage anomalies observed by GRACE satellites, with a discussion of implications for water resources.

Chapter 3: Utilization of climate and hydrologic outputs from NASA's Catchment Land Surface Model assimilated with GRACE TWSA observations, to improve spatial resolution and disaggregate the GRACE signal for the purpose of exploring the timing and magnitude of extremes throughout the terrestrial hydrologic system.

Chapter 4: Development of a multi-frequency, linear regression model to extend GRACE TWSA before and beyond the current-most available observation in an effort to estimate water storage changes back in time to the late 1940's and determine future drought recovery, solely based on TWSA relationships with rainfall.

Chapter 5: The final chapter summarizes the main results of each project, addresses potential shortcomings, and suggests future efforts towards contributing to drought research.

Chapter 2

A GRACE-based water storage deficit approach for hydrological drought characterization

As appears in:

2.1 Abstract

We supplement present-day hydrological drought characterization with a new quantitative framework for measuring the severity of regional water storage deficits based on terrestrial water storage observations from NASA's Gravity Recovery and Climate Experiment (GRACE) satellite mission. GRACE measurements are applied for hydrological drought characterization by calculating the deviation of monthly, terrestrial water storage anomalies (TWSA) from a 127-month climatology, where negative deviations represent storage deficits. Each monthly deficit explicitly quantifies the volume of water required to return to normal water storage conditions. We use the 'storage-deficit' method to quantify the severity of continuous periods of water storage deficits by combining average storage deficits with event duration. Two drought databases are referenced to identify specific meteorological drought events that occurred during the 2002-present GRACE mission lifetime in the Amazon and Zambezi River basins and in the southeastern United States and Texas regions. The storage deficit method quantifies the instantaneous and peak magnitude of water storage deficits, demonstrating the added benefits of

explicitly recognizing the beginning and end of storage deficit periods and of providing additional information about the effects of meteorological drought on regional water storage.

2.2 Introduction

The elements of drought characterization typically include drought type, frequency, duration, magnitude (including peak magnitude), severity, and areal extent of drought occurrence. Prevailing methodologies include a variety of objective (*e.g.,* meteorological and hydrological data) and subjective information (*e.g.,* drought-related articles and impact reports) to assess drought severity. Still, many definitions of drought exist, and resolving one that can be considered canonical is difficult, due to this lack of a universal definition and characteristics that are unique to each climatic regime and impact sector [*Wilhite et al.*, 2007]. More specifically, observing all of the relevant hydrological variables (*i.e.*, snow, surface water, soil moisture, and groundwater) that are necessary for characterizing hydrological drought, across the appropriate temporal and spatial scales, remains challenging.

Satellite remote sensing has emerged as a valuable tool because it offers regional-to-global coverage [*Mu et al.,* 2013]; yet, because many characterization techniques do not incorporate observations of water storage variability in all hydrological components, they cannot provide an integrated measure of the amount of water "missing" from a region during a drought episode that would be required for a return to normal conditions.

NASA's Gravity Recovery and Climate Experiment (GRACE) mission [*Tapley et al.,* 2004] provides monthly, integrated information about water storage variations throughout all components of the surface and subsurface water balance that was previously unavailable [*Wahr et. al*, 2004]. GRACE terrestrial water storage anomaly (TWSA) data have been used in a range

of hydrologic studies to estimate fluxes and water storage variations from large river basins to global scales [*e.g. Seo et al.*, 2006]; groundwater storage changes [*e.g. Rodell et al.*, 2009; *Tiwari et al.*, 2009]; freshwater discharge [*e.g. Syed et al.*, 2007]; ice mass loss [*e.g. Velicogna*, 2009]; and regional flood potential [*Reager and Famiglietti,* 2009]. *Famiglietti and Rodell* [2013] also report on the potential of the GRACE mission for further contributions to regional water management, including drought.

Currently, GRACE observations are being assimilated into land surface models [*Zaitchik et al.*, 2008], including the U.S. Drought Monitor [*Houborg et al.*, 2012]. While these models enable downscaling and decomposition of GRACE data into water storage components, simulation of the severity of drought events is limited by the model physics, model structure, and the accuracy of additional model parameters and meteorological forcing data [*Long et al.*, 2013]. An independent, observation-based water storage deficit is desirable for drought characterization because it is not limited by model assumptions or access to auxiliary datasets. In addition to the potential for advancing drought characterization, it also creates the opportunity for improving models and for new applications including forecasting drought initiation and recovery.

Previous works from *Yirdaw et al.* [2008], *Chen et al.* [2009], *Leblanc et al.* [2009], *Frappart et al.* [2012], and *Long et al.* [2013] examined individual, regional scale droughts using gravity-based measures of water storage variations from the GRACE mission; however, these studies have not yet placed GRACE observations into a consistent drought characterization framework for quantifying drought severity in terms of the water absent from a region that can be applied to a variety of regions around the world.

We demonstrate that GRACE can contribute to regional drought characterization by measuring water storage deficits in a previously-identified, drought-stricken area, and that the

duration and magnitude of the deficit can serve as new metrics to help quantify hydrological drought severity. We present gravity-based measurements of water storage anomalies during recent, well-documented meteorological droughts (defined as extended periods of precipitation deficits), including those in the Amazon and Zambezi River basins, and the Texas and Southeastern regions of the United States. We use GRACE to further characterize the effects of meteorological drought within the hydrological system, to explore how hydrological drought (generally defined as extended periods of water storage deficits) may be better characterized, and to estimate the associated regional water storage deficit. We expect that these results can ultimately contribute to a comprehensive framework for drought monitoring [*Famiglietti and Rodell,* 2013].

2.3 Data

GRACE observes monthly changes in Earth's gravity field caused by mass redistribution, which, over land and after removal of the atmospheric contributions, are attributed primarily to the movement of water in various surface and sub-surface hydrologic reservoirs [*Wahr et al.,* 2004]. Here we use the University of Texas Center for Space Research (CSR) Release 5.0 (RL05) monthly, global, one-degree gridded and scaled GRACE land water storage data, which are expressed in centimeters of equivalent water thickness [*Landerer and Swenson,* 2012]. Data are available at http://grace.jpl.nasa.gov (refer to *Swenson and Wahr* [2006] for post-processing details). GRACE data require scaling to restore true signal amplitude attenuated by data processing [*Velicogna and Wahr,* 2006]; therefore, scaling factors, based on the Community Land Model (CLM) v4.0 [*Oleson et al.,* 2008] are provided and multiplied by the un-scaled GRACE data following *Landerer and Swenson* [2012]. A three-month, low-pass filter is also

applied to reduce noise before converting storage anomalies from centimeters of water equivalent height to cubic kilometers of water volume.

Prior work by *Long et al*. [2013], showed GRACE to be a valuable tool to link meteorological drought to hydrological drought. Accordingly, we use two drought databases to identify the presence of meteorological drought in each region and to border our two U.S. study regions. First, maps of drought conditions from the United States Drought Monitor [*U.S. Drought Monitor*, 2013] were used to define the boundaries of regions subjected to major meteorological drought during the GRACE mission lifetime. The maximum areal extent of D2 (Severe) to D4 (Exceptional) drought severity classes was used to delineate boundaries for the 2007-2009 Southeastern United States and 2010-2013 Texas region droughts (see Figure 1). Second, we selected watersheds based on drought information from the Office of U.S. Foreign Disaster Assistance (OFDA)/Centre for Research on the Epidemiology of Disasters (CRED) International Emergency Events Database [*EM-DAT*, 2013]. This archive identified major meteorological droughts that occurred within the world's large river basins during the GRACE period of record. The Amazon and Zambezi River basins were subsequently selected for analysis (Figure 1).

Study area masks were used to calculate monthly regional-average water storage volume anomalies (in km^3) by multiplying GRACE storage anomalies with the regional mask area (see Table 1a for mask areas). Gridded, time-invariant measurement and leakage errors were provided with the GRACE data set, and applied for the calculation of the following total monthly regional average errors, based on methodology from *Landerer and Swenson* [2012]: ±11.25 mm/69.12 km^3 (Amazon), ±19.06 mm/25.55 km^3 (Zambezi), ±14.55 mm/11.33 km^3 (Texas), ±16.02 mm/11.75 km^3 (Southeastern United States). These errors offer a measure of the relative

GRACE sensitivity to water storage variations in different regions. Larger areas have smaller relative error (per signal), directly related to the effective spatial resolution of GRACE satellites.

2.4 Water Storage Deficits and Hydrological Drought Characterization

We computed a 127-month climatology (January 2003-July 2013) for the GRACE TWSA time series in each study region by averaging the TWSA values of each month of the GRACE record (*e.g.*, all Januaries in the ~10 year record are averaged). This climatology represents the characteristic variability of water storage and serves as a baseline for identifying the occurrence and severity of water storage deficits. We recognize that a climatology of at least 30 years is preferable; nevertheless, a consistent measure of water storage with global coverage from the GRACE mission is currently the best available. While the GRACE record is relatively short, note that in this paper we are proposing a method for drought characterization that can be continuously updated as the GRACE record length grows.

Water storage deficits were calculated as negative residuals after subtracting the GRACE climatology from the GRACE TWSA time series. This is distinct from former work by *Long et al*. [2013] where they subtracted the mean (constant) gravity field from the long-term monthly, GRACE-derived TWSA. Our calculated residual time series depicts the substantial deviation from the normal annual or seasonal cycle that can then be considered a true deficit and are used to distinguish between relatively dry (negative residuals shown in Figure 1) and wet (positive residuals, not shown) conditions in the four study regions. For convention, deficits and severity are denoted here with a negative sign.

Monthly negative residuals represent regional water storage deficits, providing a direct measure of the magnitude, M (km^3), of the volumetric departure from "normal" (climatological)

16

hydrological conditions, or accordingly, the volume of water required, at any point in time, to return to normal hydrological conditions. *M* also serves as a rolling, monthly measure of the instantaneous deficit magnitude. We calculate one standard deviation of the residual time series and plot it above and below the climatology for reference.

Any deficit period lasting three or more continuous months is designated as an event, which allows us to quantify the hydrological impacts of a meteorological drought occurrence on an event-by-event basis. We designate a hydrological drought as a deficit event that coincides with a widespread, regional meteorological drought [refer to Table 1 for all drought characterization variables].

Figure 1 displays plots of monthly, regional-average GRACE TWSA's (black line) with error bars, GRACE TWSA monthly climatology (blue dashed line) with confidence bounds (light purple shading), and water storage deficits (green-shaded area, scale on right axis) in the left panel. The right panel highlights months with the largest peak magnitude for each study region (refer to Table 1d) of the residual time series in the left panel. Deficits are presented on one-degree grids, masked for each study region, and are standardized by dividing each value by the standard deviation of the residual time series for each grid cell. These maps offer a spatial perspective on the magnitude of negative departures from normal, monthly climatological conditions.

To capture the combined impact of water storage deficits and duration, we define the severity, $S(t)$ (km^3 months), of each deficit event as the product of the average deficit since the onset of the deficit, $\overline{M}(t)$ (km^3) and the duration $D(t)$ (months) since deficit onset, or:

$$S(t) = \overline{M}(t) \times D(t) \qquad \text{(Figure 2.1)}$$

17

Additionally, at the termination of an event (*i.e.*, once the monthly residual is no longer negative), the total event severity, calculated at the end of the event as *S,* is equal to $\overline{M}$ x *D* for the total months of continuous storage deficits (Table 1g). Note that *S,* $\overline{M}$, *P*, and *D* can only be determined historically, and will be helpful for comparison with documented drought occurrences, while *M* serves as the instantaneous measure of the magnitude of the deficit event.

2.5 Results

Table 1 provides a summary of results for each region. While Figure 1 shows all deficit periods, only those lasting for three or more consecutive months are listed in the table. Figure 2 features the severity time series with each uninterrupted deficit period labeled with its corresponding total severity value (also listed in Table 1g).

2.4.1 Amazon

There were seven occurrences of GRACE-identified water storage deficit events in the Amazon basin (Figures 1a, 2a; Table 1). The largest peak magnitude occurred in July 2005 with 512 km^3 of storage below climatological conditions. Deficits in 2004, 2005, and 2010 had similar total severities (-2547, -3627, and -3289 km^3 months, respectively), with durations of 9 and 13 months. These results are consistent with the OFDA/CRED EM-DAT database, which documented three major meteorological droughts affecting countries within the Amazon River basin (in 2004, 2005, and 2010) [*EM-DAT*, 2013].

2.4.2 Zambezi

The Zambezi River basin experienced the longest deficit event of the areas studied (60 months: from January 2003 to December 2007). It is also the one with the greatest total severity (-5280 km^3 months) (Figures 1b, 2b; Table 1c). The region's peak deficit of 222 km^3 below climatology occurred in April 2005. The OFDA/CRED EM-DAT database documented meteorological droughts for territories sharing the Zambezi River basin in 2005 and 2007 [*EM-DAT*, 2013], which is considerably shorter than the 5 years of nearly continuous water storage deficits identified using GRACE.

2.4.3 Texas

There were four GRACE-identified deficit periods within the Texas region (Figures 1c, 2c; Table 1c). One month of surplus storage interrupted events from November 2008 to September 2009. The largest peak magnitude occurred during the most recent event, which began in October 2010 (-68 km^3 in January 2013). The U.S. Drought Monitor detailed two major, widespread meteorological drought periods in its South region in 2006 and from 2011-2013, which is consistent with storage deficits observed with GRACE.

2.4.4 Southeastern United States

The Southeastern United States experienced three water storage deficit events (Figures 1d, 2d; Table 1c). Two months of surplus storage punctuated the events from October 2010 to March 2013 (April and May 2011). The peak magnitude for this region was -66 km^3 in November 2007. U.S. Drought Monitor time series show two major meteorological drought periods during the GRACE record from 2007-2009 and 2010-2013, which, as above, is

consistent with storage deficits identified by GRACE from February 2008-November 2008 and July 2011-March 2013.

2.4.5 Using deficits to estimate drought recovery

The monthly deficit (M) quantifies the volume of water required to recover from below normal water storage conditions. One of the benefits of the storage-based approach is that the time evolution of storage deficits, including their rates of increase or decrease, can be evaluated by estimating the time derivative of the deficit, dM/dt. This is done as a backwards difference calculation:

$$\frac{dM}{dt}(t_i) = \frac{M(t_i) - M(t_{i-1})}{t_i - t_{i-1}}, \text{ for I = 1:N} \qquad \text{(Figure 2.2)}$$

where M is the monthly deficit, t is time, and N is the length of the GRACE record. Since the GRACE record is short and may contain few instances of drought (or drought recovery), we have assumed that the entire dM/dt time series (not only those points in previous drought recoveries) can be used to represent a range of typical dM/dt values. As an example, we calculate the dM/dt distribution and statistical percentiles of the empirical (Kaplan-Meier) cumulative distribution (eCDF) of dM/dt within the Texas region, which follows a standard normal distribution according to a one-sample Kolmogorov-Smirnov test. We select, for demonstration, the 95th percentile (2 standard deviations) of the eCDF to represent the maximum positive rate of change for deficits, and the 68th percentile (1 standard deviation) to represent the average positive rate of change for deficits, for any deficit month.

The quotient of a monthly deficit value and either the maximum or average rate of change yields the minimum or average time to recovery, allowing us to assign a likely time range for recovery for every month through the end of the event. Based on the 95th (11 km^3/month) and

68th (3 km^3/month) percentiles of the eCDF (Figure 3c, inset), the minimum and average times to recovery from the July 2013 deficit (-38 km^3) are ~3 and ~13 months, respectively (Figure 3c).

2.6 Discussion

The GRACE-based drought characterization framework presented here offers three key contributions to drought characterization efforts: a framework that provides additional information about the effects of meteorological drought; specifically, how much water is missing from a region during a drought, a clear identification of water storage deficits and quantification of their severity with an observation that integrates both surface and subsurface storage, and a consistent method for severity calculation that can be applied globally.

Instances where GRACE deficits occurred without a meteorological drought (*see Table 1*) likely suggest that GRACE deficits must be greater than some regional threshold associated with typical variability. The delineation of that threshold could be deduced from Table 1, and with a longer GRACE time series these thresholds will become more established. There were no situations for which there is a wide-spread meteorological drought within a basin, and no significant water storage deficit occurs in GRACE data.

Differences in the timing of meteorological drought and GRACE deficits may be due to inherent lags within the hydrologic system (*i.e.*, subsurface water storage can be slow to react to precipitation changes). Our analysis shows that it is the severity metric (S), and not the magnitude or duration alone, that is most associated with reports of widespread, catastrophic meteorological drought, and corresponds best with major, region-wide meteorological droughts [Table 1h].

There is currently very little understanding of subsurface water supply (*e.g.*, root zone moisture and groundwater, described as the saturated zone extending to the bedrock); hence, this is an important feature captured by our drought characterization framework. For example, the response of groundwater is slower compared to changes in rainfall and snowmelt [*Eltahir and Yeh*, 1999]; hence, GRACE-observed deficits within a region may appear later and persist longer in these subsurface reservoirs. Because many common drought metrics tend to be based on the accumulation of precipitation deficits or anecdotal accounts of events, they cannot see the extent of drought influence on subsurface hydrology. Though surface storage may be quickly (seasonally) replenished, deficits in the subsurface leave the region vulnerable to future droughts. When the surface supply is once again depleted and subsurface supply is still inadequate, then the consequences can be severe. As we did not separate the storage components, it is not evident how much water is explicitly missing from the subsurface; however, since the integrated signal observed deficits, groundwater in these regions is likely declining as well.

With this framework, it is possible to monitor the intra-seasonal persistence of total water storage deficits and surpluses. This presence, even during a wet season, indicates that an inter-annual drought event is still occurring (though maybe not visible) and may not be resolved in the coming year. This offers potential for drought forecasting for the upcoming dry season, and for improving drought monitoring systems [*Famiglietti and Rodell*, 2013]. Understanding the time evolution of deficit severity is also important for drought monitoring efforts. An event with similar severity but, for example, a shorter time evolution than another means that the deficits accelerated (*i.e.*, deficits worsened) more rapidly than another, more slowly developing, event.

In the GRACE-based framework described here, the selection of an averaging area and an understanding of relevant hydrological processes are important in characterizing the intensity

of one regional event relative to others. Regional land characteristics, regional land-surface and atmospheric coupling, and regional water management decisions influence drought severity. Our quantification of the timing and severity of water storage deficits is described in a manner that can be quickly applied as new GRACE data arrives. Ongoing work will explore using GRACE data to identify drought independently of meteorological drought indices and boundaries, in an effort to provide a truly independent characterization of drought occurrence and severity.

2.7 Acknowledgements

A. Region	B. No. of events ≥ 3 months	C. Time span of each event	D. Peak Magnitude (P) km³	E. Duration (D) (months)	F. Average water storage deficit km³	G. Total Severity (S) (km³ months)	H. Coincides with a meteorological drought?
Amazon Area: 6,140,600 km²	7	Jan-03 to Jun-03	-407 (Mar-03)	6	-277	**-1662**	N
		Nov-03 to Jul-04	-442 (Apr-04)	9	-283	**-2547**	Y
		Dec-04 to Dec-05	-512 (Jul-05)	13	-279	**-3627**	Y
		Feb-07 to Oct-07	-235 Apr-07)	9	-129	**-1161**	N
		Feb-10 to Feb-11	-370 (May-10)	13	-253	**-3289**	Y
		Aug-11 to Oct-11	-23 (Oct-11)	3	-19	**-57**	N
		Aug-12 to Jan-13	-175 Nov-12)	6	-109	**-654**	N
Zambezi 1,340,600 km²	1	Jan-03 to Dec-07	-222 (Apr-05)	60	-88	**-5280**	Y
Texas Area: 778,770 km²	4	Nov-05 to Aug-06	-28 (Jan-06)	10	-17	**-170**	Y
		Nov-08 to Apr-09	-25 (Feb-09)	6	-15	**-90**	N
		Jun-09 to Sep-09	-21 (Aug-09)	4	-11	**-44**	N
		Oct-10 to Jul-13	-68 (Jan-13)	34	-43	**-1462**	Y
Southeastern United States Area: 733,760 km²	3	Dec-05 to Mar-09	-66 (Nov-07)	14	-42	**-588**	Y
		Oct-10 to Mar-11	-21 (Jan-11)	3	-24	**-72**	N
		Jun-11 to Mar-13	-60 (Jun-12)	6	-15	**-90**	N

Table 2.1. Summary table of GRACE-identified hydrological drought events: A. region name with boundary area; B. number of events; C. time span of each event; D. peak magnitude (P, the largest value of the deficit, M, that occurs during a hydrological drought in km³); E. duration (D, the number of months of continuous storage deficits); F. average water storage deficit (km³); G. total severity (S, km³ months). A hydrological drought period that corresponds with a major, documented meteorological drought is indicated with a 'Y' (column H) and the row is shaded. Only events lasting three months or longer are listed.
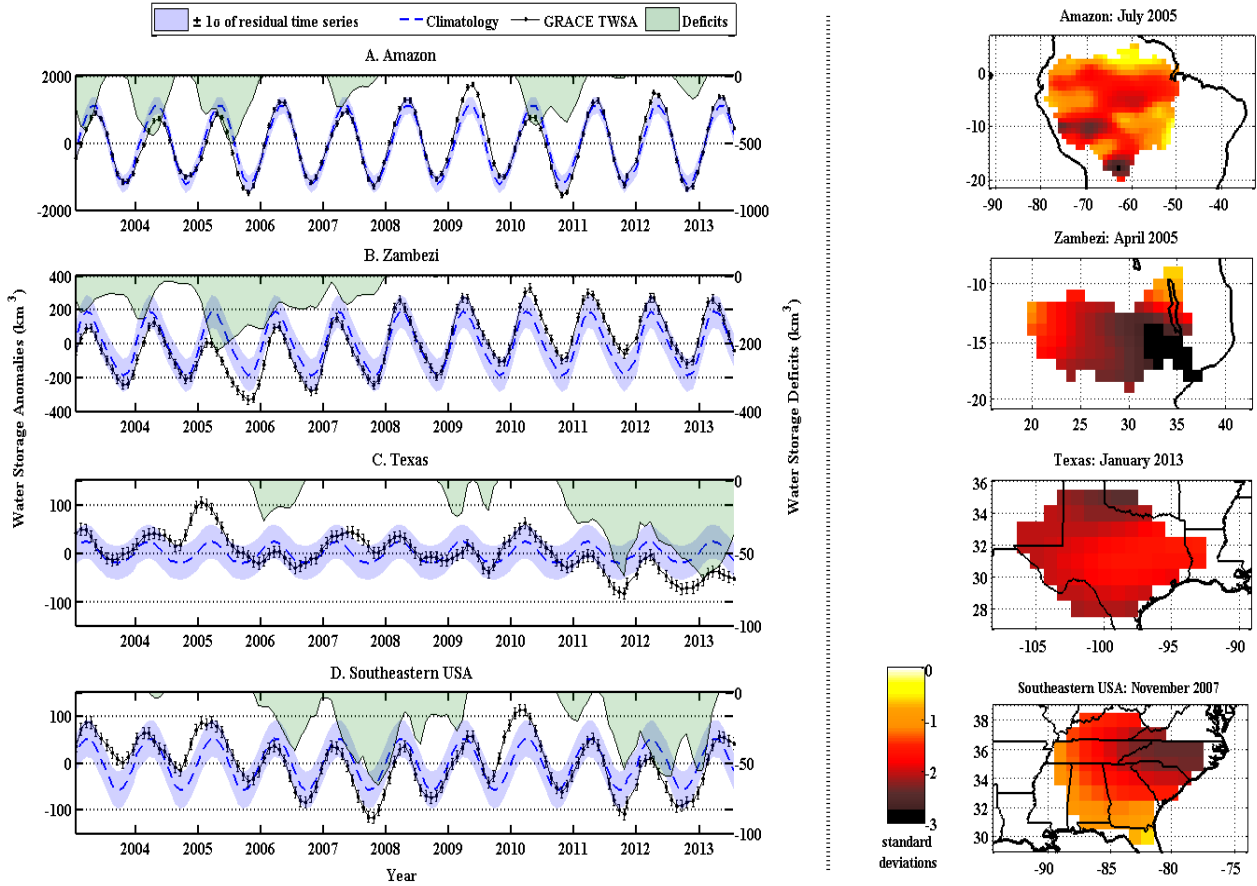
Figure 2.1. GRACE-observed deficits for all study regions. *Left panel*: GRACE-observed water storage anomalies and deficits for each study region. Black lines: regional, spatial average storage anomalies with error bars (km^3); Blue dashed lines: monthly climatology and; Green-shaded areas: water storage deficits (km^3). Light purple shading around the climatology represents ± one standard deviation of the residual time series. *Right panel*: Regional maps of one-degree, gridded GRACE-identified water storage deficits on a regionally standardized scale, highlighting months with the largest peak magnitude for each study region. A. Amazon, July, 2005; B. Zambezi, April, 2005; C. Texas, January, 2013; and D. Southeastern United States, November, 2007.
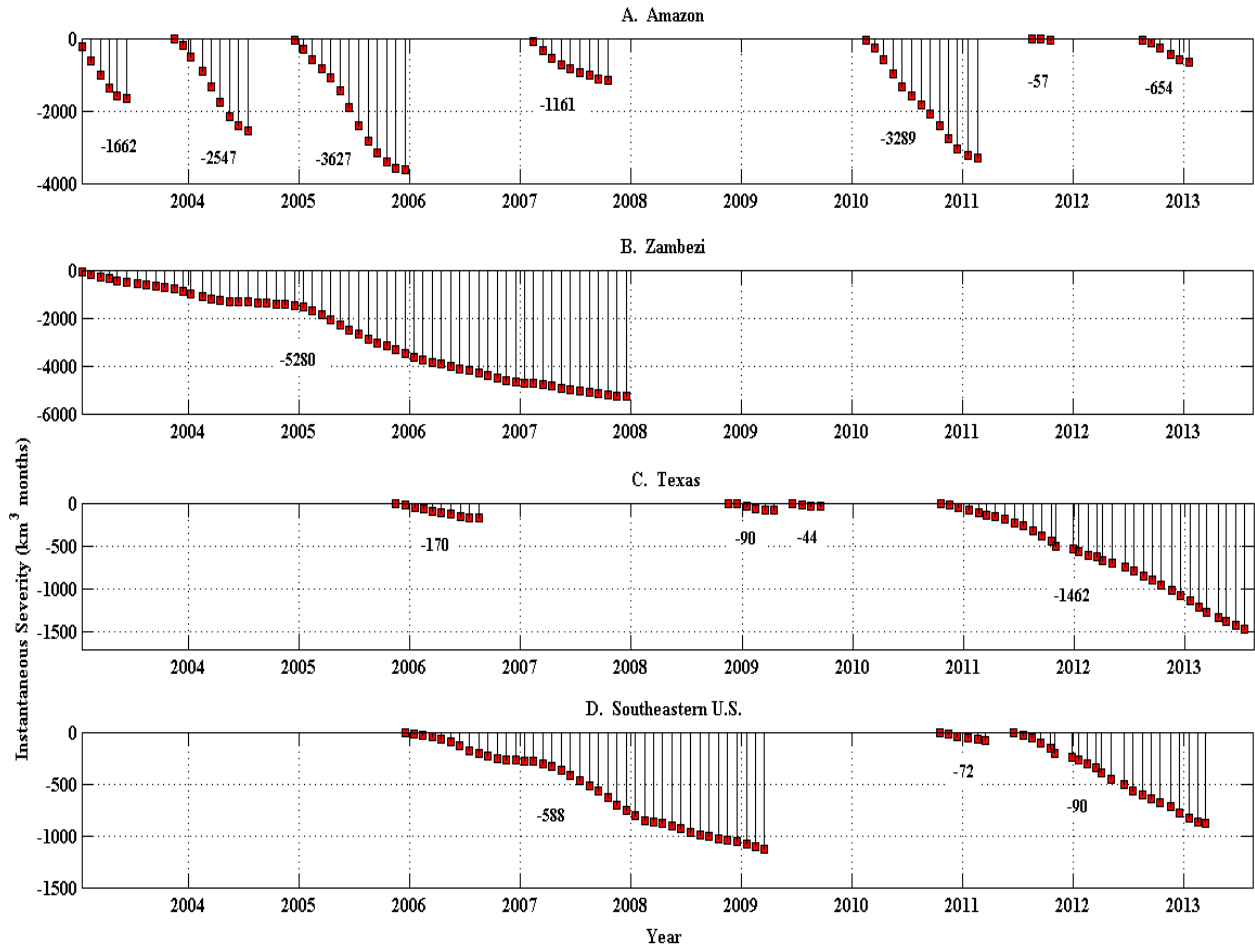
Figure 2.2. Instantaneous and total severity for GRACE-observed, regional average water storage deficits: A. Amazon, B. Zambezi, C. Texas, and D. Southeastern United States. Total severity (S) values for each event are given in bold (km^3 months).
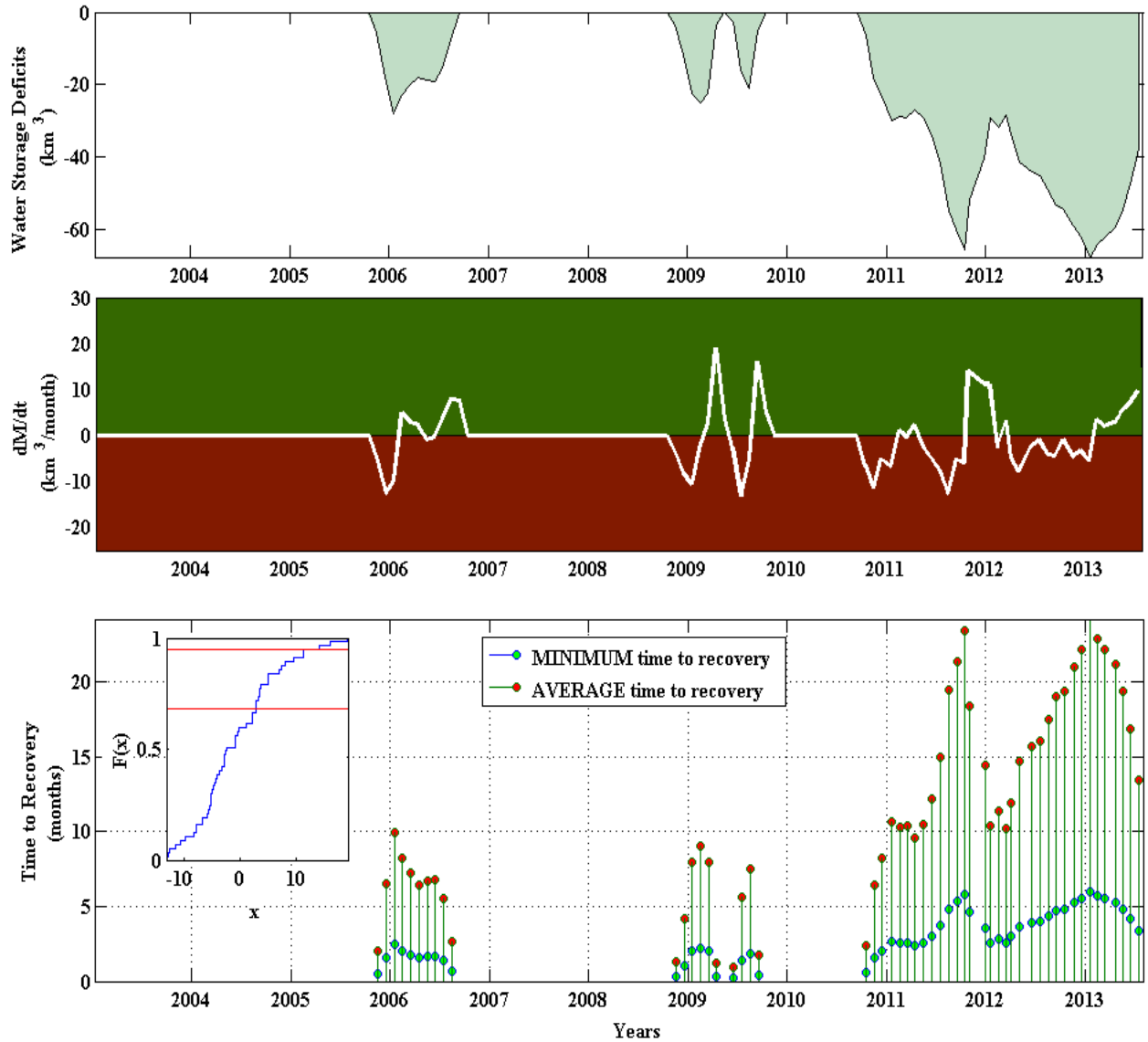
Figure 2.3. Estimated time to recovery for the Texas region: A) GRACE water storage deficits (km^3); B) monthly rate of change of deficits (*dM/dt*) in km^3/month; and C) the minimum and average times to recovery. *Inset*: empirical cumulative distribution of *dM/dt*; the 68th and 95th percentiles (red lines) are used to determine the average and minimum time to recovery; all for January 2003 through July 2013.

Chapter 3

Using model-assimilated GRACE water storage anomalies to explore terrestrial hydrologic extremes plus an assessment of model degradation in successive months following the last assimilated observation

3.1 Introduction

Traditionally, the analysis of hydrologic extremes has involved statistical assessments of long-term (30+ years) climatic and hydrological datasets to determine drought and flood occurrences, severity, and recurrence intervals. Contemporary extremes analysis and monitoring has not deviated much from its roots, though it has obtained a wealth of new tools for measuring land and atmospheric variables, namely satellite remote sensing products and advanced computer modeling abilities. The previous chapter explored ways that GRACE can be utilized to quantify water storage deficit and surplus on a global scale, features that are currently only attainable with GRACE satellite observations.

While GRACE terrestrial water storage anomaly (TWSA) data contribute to an improved understanding of how terrestrial water storage responds to climate change and variability [*Syed et al.*, 2008], the application of GRACE data for hydrologic extreme analyses is not without its limits. Three prevailing limitations to the direct application of GRACE satellite observations for quantification of extremes are coarse spatial resolution (one degree), the aggregation of multiple water storage components into one, integrated value for each grid cell, and latency in data acquisition (2-5 months lag), which may not always prove useful for certain applications, such as water resource management. For preliminary quantification of regional-average total water storage, GRACE observations are imperative, yet we can undoubtedly benefit from higher

28

resolution data sources, temporal and spatial, observed and modeled [*Wood et al.*, 2011; *Forman et al.*, 2012].

Computer modeling of land-atmospheric processes and interactions offers the potential for a level of temporal and spatial resolution beyond the capacities of most *in situ* observation networks. A general land surface model (LSM) is constructed to describe, propagate, and output the dynamic relationships between hydrological, atmospheric, and land surface properties throughout the terrestrial system generally by modeled physics derived from empirical relationships. *Overgaard et al.* [2006] states that even though many LSMs include detailed descriptions of vegetation and soil moisture parameters, the interactions between deeper, subsurface (*i.e.,* groundwater), root zone and surface water, and lateral surface and subsurface flows, are typically disregarded. This causes these models to fail to produce accurate results in areas where subsurface interactions are important.

The Catchment Land Surface Model (CLSM) was developed at the NASA Goddard Space Flight Center with a goal of improving the handling of the sub-grid horizontal structure of land surface hydrological processes, by explicitly accounting for sub-grid soil moisture variability and its effects. Unevenly shaped hydrologic catchments, with boundaries defined by topography, serve as the primary elements of the land surface instead of quasi-rectangular atmospheric grid elements, though, as in our application, regular grids can be applied [*Koster et al.*, 2000]. The land surface of the CLSM is divided into topographically-defined catchments with an average area of approximately 4000 km^2, where water is redistributed spatially and vertically based on the topography of each basin or watershed [*Li et al.*, 2012]. The model's hydrologic processes are based on each catchment's topographical statistics. Refer to *Ducharne*

et al. [2000] and *Koster et al.* [2000] for more detailed discussion on the philosophy, configuration and implementation of the CLSM.

Data assimilation, the process of merging measurements with model predictions, to maximize spatial and temporal coverage, consistency, resolution, and accuracy, addresses a necessity for the improvement of land-surface model outputs that assume uniform topographic and hydrologic characteristics at the grid scale level, a feature that often leads to unrealistic fields of hydrological components like runoff, river flow, and groundwater [*Reichle et al.*, 2002b]. It involves the spatial pairing of satellite data with model-defined boundaries with either global/regional grid cells *(i.e.*, Global Land Data Assimilation System; *Rodell et al.*, 2004) or watershed-defined domains (*i.e.*, the CLSM).

Assimilation has been shown to improve model outputs, in several cases, decreasing RMS errors and significantly increasing the correlation between simulated and observed variables [*Reichle et al.*, 2002a]. *Zaitchik et al.* [2008] discusses several advantages of CLSM-GRACE data assimilation. For example, the pairing of GRACE estimates with a watershed-defined CLSM domain allows for area-accurate assimilation within hydrologically defined basins. Additionally, the saturated, unsaturated, and wilting segments of the model provide a physically-based mechanism for weighting the hydrologic effects of an assimilated GRACE observation across the modeling element, which provides rationale for spatially distributing the properties of assimilation at scales less than one degree.

Houborg et al. [2012] established that data assimilation is the key to realizing the full potential of GRACE TWSAs for hydrological applications, because it enables spatial and temporal downscaling, extrapolation to near real time, and vertical disaggregation into groundwater, root zone and surface soil moisture components. The authors state that their

outcomes pointed towards moderate, but statistically significant, improvements to the hydrological modeling skill of the CLSM across major parts of the United States. Additionally, *Li et al.* [2012] recognized the potential for GRACE data to improve the simulation of land surface processes for drought monitoring applications.

The work discussed in this chapter combines modern satellite- and computer model-derived datasets with conventional statistical methods to describe how water storage varies through several levels of the terrestrial hydrologic system (*e.g.*, snow, surface and root zone soil moisture, and groundwater). This analysis uses disaggregated water storage outputs from the CLSM, assimilated with GRACE data, to explore the potential usages of data assimilation for characterization and monitoring of hydrologic extremes (*i.e.*, flood and drought). We explore the benefits of data assimilation by exploring similarities and disparities between CLSM assimilation outputs (CLSM-DA), GRACE observations (GRACE), and CLSM Open-loop runs (CLSM-OL; obtained by running the CLSM without any data assimilation), focusing on four areas in the United States. Further, we provide an evaluation of CLSM's performance between assimilation updates.

3.2 Data

3.2.1 GRACE Satellite Data

The Gravity Recovery and Climate Experiment (GRACE) comprises of a pair of satellites flying, in tandem, at over 400 km altitude, spaced about 220 kilometers apart. Distance variations between the two satellites, as they approach a mass anomaly, are measured using a K-band Ranging System (KBR), which provides precise (within 10 μm) measurements of the distance change between the two satellites needed to measure fluctuations in gravity [*Tapley et al.*, 2004].

The corresponding time variations in the gravity field are used to determine changes in the Earth's mass distribution at horizontal resolutions greater than 150,000 km^2, with higher measurement accuracy at larger spatial scales [*Wahr et al.*, 2004]. We attribute the monthly to decadal temporal changes in the gravity field to mass redistributions in the atmosphere, ocean and continents. These measurements of changes in total terrestrial water storage (TWSA) represent the mass movement of regional water storage over time.

The GRACE dataset used for this project is the same as in the work detailed in Chapter 2 (*i.e.*, monthly, global, one-degree gridded, scaled GRACE land data product), processed by the Texas Center for Space Research [CSR; version CSR-RL05]). The time period for this project is from April 2002 to January 2014. Refer to *Swenson and Wahr* [2006] and *Wahr et al.* [1998] for post-processing details and to *Landerer and Swenson* [2012] for particulars on signal restoration, scaling, and regional error calculation. Corrections for postglacial rebound have also been applied to the data following *Chambers et al.* [2010].

For temporal analyses, GRACE data were spatially averaged for four United States National Climate Assessment (NCA) regions: the Southeast (Region 2), Northern and Southern Plains (Regions 4 and 5), and Southwest (Region 7), with total, regional TWSA errors of 1.44, 0.85, 1.21, and 0.77 cm, respectively. These zones represent dominant climate regions throughout the country (refer to Figure 1 for an NCA zone map). Area masks were used to spatially average monthly storage components. Time series and maps of "residual" water storage were calculated following methodology in *Thomas et al.* [2014], where surplus and deficit storage is determined by removing the monthly climatology from the original storage time series.

3.2.2 AMSR-E Soil Moisture Dataset

The Advanced Microwave Scanning Radiometer for the Earth Observing System (AMSR-E) dataset contains global monthly-mean surface soil moisture average values (1x1 degree grid cells). AMSR-E/Aqua Level-3, global, monthly, surface soil moisture averages (Product: AMSR_E_L3_DailyLand; *Njoku et al.*, 2004) were used as independent measures to evaluate the effectiveness of the CLSM-GRACE assimilation. AMSR-E soil moisture retrievals represent vertical sampling depth in the top ~1 cm of the soil column, averaged over the horizontal retrieval footprint area. The actual sampling depth will vary with the amount of moisture in the soil. Soil moisture deeper than ~1 cm below the surface may not be sensed by AMSR-E [*Njoku et al.*, 2004]. Soil moisture values are in g/cm^3 with an accuracy of 0.06 g/cm^3 [*Njoku et al.*, 2003].

Data were downloaded from the Goddard Earth Sciences (GES) Data and Information Services Center (DISC) for the time range from October 2002-September 2011. NCA region masks were used to calculate monthly, regional-average AMSR-E soil moisture time series. Values for missing months (October-November 2003 and February 2010) were interpolated by way of a 2-D, spline interpolation. I divided monthly soil moisture values by the time series' standard deviation to standardize AMSR-E data so they can be directly compare with soil moisture outputs from the CLSM. I also applied a 4-month, low pass filer to smooth the time series.

3.2.3 CLSM Dataset

Original CLSM outputs were converted from millimeters of water storage per day to storage anomalies in centimeters per month. CLSM output variables used in this analysis are:

33

total grid cell water storage (TWS), snow water equivalent (SWE), surface moisture (SFMC, 0-0.2 m), and root zone moisture (RZMC, 0.2-10 m). We also calculate storage below the root zone (Below RZMC) by subtracting SWE, SFMC, and RZMC from the TWS time series. The term 'Groundwater' will be used interchangeably with 'Below RZMC'. TWS is the only variable used from the CLSM-OL run.

3.3 CLSM Methodology

3.3.1 CLSM Physical Processes

CLSM is a physically based, apportioned land surface model whose strength lies in its ability to simulate unconfined groundwater storage variations, typically 2-3 meters below the terrestrial surface [*Houborg et al.*, 2012]. This groundwater layer is an essential variable to be included in a land model if we are to generate terrestrial water storage variations that are analogous to those measured by GRACE satellites. The TOPMODEL framework of *Beven and Kirkby* [1979] is utilized to establish root zone soil moisture distributions from the morphology of the catchment and from bulk soil moisture prognostic variables. TOPMODEL formulations allow for the calculation of both the saturated fraction and the baseflow of a watershed in addition to translating the mean watershed water table depth and a probability density function of combined topographic and soil properties [*Koster et al.*, 2000; *Gascoin et al.*, 2009]. At the core of TOPMODEL are three essential assumptions:

1) *The water table is nearly parallel to the soil surface so that the local hydraulic gradient is close to the tangent of the local slope angle,*

2) *The saturated hydraulic conductivity declines exponentially with depth,*

3) *The water table is recharged at a spatially uniform and steady rate with*

respect to the response timescale of the watershed. As such, recharge and

baseflow are balanced in a series of steady states [Koster et al., 2000].

CLSM follows the founding work of *Famiglietti and Wood* [1994], who were the first to include the TOPMODEL framework in a land surface model, to relate water table distribution to basin topography. Sub-catchment heterogeneity of soil moisture is modeled by dividing the catchment into dynamic fractions of saturated, unsaturated, and wilting areas, each ruled by equations appropriate for its soil moisture status [*Zaitchik et al.*, 2008]. The distribution of soil moisture in the root zone allows the catchment to be portioned into these distinct regimes [*Koster et al.,* 2000; *Ducharne et al.*, 2000]. These surface fractions exchange heat separately with the underlying ground layer, which also exchange heat with lower ground layers. A three-layer snow model, detailed in *Lynch-Stieglitz* [1994], is also coupled to the catchment model to determine snow melting, refreezing, changes in snow density, snow insulating properties, and physics related to the growth and ablation of snow [*Stieglitz et al.*, 1997].

CLSM's primary prognostic variable is the catchment deficit, defined as the average depth of water that would need to be added to bring the catchment to saturation [*Ducharne et al.*, 2000]. The equilibrium vertical distribution of soil moisture is then diagnosed on the basis of the catchment deficit and soil parameters. This distribution includes an implicit water table, located at the depth of equilibrium saturation. Additional prognostics include reservoirs of surface excess moisture and root zone excess moisture that yield an approximate representation of non-equilibrium vertical conditions such as infiltration fronts [*Koster et al.,* 2000]. The surface excess moisture reservoir, comprised of the first two centimeters of the soil layer, is small relative to both root zone excess (the soil layer from 2-100 cm) and the catchment deficit.

3.3.2 CLSM-GRACE Data Assimilation

For this study, we focused on the assimilation of GRACE satellite observations with NASA's CLSM. The CLSM-DA time series is from January 2003 to April 2014. Outputs are posted onto 0.25-degree grid cells for the intercontinental United States (domain: -126.875 23.875, -66.125 51.625), including portions of Canada and Northern Mexico. This gridded analysis is an interpolation of catchment tiles to a model grid. For the assimilation, the model-generated terrestrial water storage moisture components are corrected toward the GRACE observational estimate with the degree of correction determined by the levels of error associated with each using and Ensemble Kalman Smoothing Filter method (EnKS). *Zaitchik et al.* [2008] developed the EnKS scheme to specifically assimilate GRACE-O into the NASA Catchment Land Surface Model in the Mississippi basin. Monthly GRACE anomaly fields are converted to absolute values by adding the time-mean total water storage field from the CLSM-OL output. Assimilation increments are calculated based on the relative uncertainty in the model and the observations where an iterative smoother is applied to handle GRACE's monthly temporal resolution. These increments are applied directly to the column-integrated prognostic variable (the catchment deficit) and the primary non-equilibrium prognostic (the root zone excess moisture), without need for arbitrary vertical disaggregation.

3.4 Results

In section 3.4.1 I showcase how assimilation improves the spatial resolution of the CLSM-OL for several extreme events across the United States. Section 3.4.2 explores the vertical disaggregation of CLM-DA variables for the four NCA regions, with emphasis on occurrences of hydrologic extreme events. Section 3.4.3 compares SFMC from the CLSM with

surface moisture from the AMSR-E satellite and provides an evaluation of CLSM degradation in months following assimilation for our study regions. All results are presented in units of centimeters of equivalent water storage.

3.4.1 Spatial Resolution Improvement

Four major hydrologic extreme events, that occurred within the GRACE period of record, are displayed in Figure 2: Northern California floods (January 2006, Figure 2a), Northern Plains floods (June 2011, Figure 2b), Southeastern drought (December 2007, Figure 2c), and Central U.S. drought (October 2012, Figure 2d). GRACE (left panels) captures these major events yet lacks the spatial resolution to pinpoint the severest areas. CLSM-OL (middle panels) also captures events though it over estimates the severity and spatial extent of droughts and underestimates flood events, compared to GRACE. CLSM-DA (right panels) is a suitable middle ground between GRACE observations and CLSM-OL because it captures events with greater resolution than GRACE and values that more closely match the satellite observations.

3.4.2 Vertical Disaggregation

Figure 3 shows the vertically disaggregated components of the residual CLSM-DA time series (TWS, Below RZMC, RZMC, SFMC, and SWE) and GRACE residual TWSA (gold squares), for the four study zones. Regional R^2 values, between GRACE and CLSM-DA TWSA, ranged from 0.83-0.88, with the best match in the Southern Plains and worst in the Southeast. Overall, CLSM-DA TWSA deficits are comparable to those from GRACE though several events are underestimated in the Southwest and Northern Plains. The 2007 event in the Southeast was overestimated by 3-4 cm. Further, TWSA surplus months closely matched GRACE with the

exception of underestimation in the beginning of the record in the Southwest and slight overestimation in 2005 in the Southern Plains. Additionally, the major surplus event in the Northern Plains started in 2009 with GRACE but CLSM-DA did not begin to show substantial surplus until 2010.

The plots reveal timing differences between changes in water stores. For example, in the Southern Plains, SFMC declines lead RZMC and Groundwater by two to three months. In all regions, there are numerous occasions where RZMC residuals lead Groundwater changes by one to three months. Southwest SFMC and RZMC showed a slight surplus in late 2013 while Groundwater remained deficient. RZMC also shows the most monthly variation between positive and negative values out of the storage components. In the Northern and Southern Plains, RZMC recovers for one to two months on several occasions during extended deficit periods while the other stores remained negative. In the Southwest, Southeast, and Northern Plains, peak SWE residuals were often matched or immediately followed by an instance of surplus or deficit.

3.4.3 CLSM-DA Performance Assessment

I compared SFMC (0-2 cm layer) from CLSM-OL and CLSM-DA with an independent measure of surface soil moisture content observed by AMSR-E/Aqua to assess whether assimilation truly improved modeled moisture outputs. Time series of results for the AMSR-E period of record (October 2002-September 2011) are displayed in Figure 4. Figure 5 shows spatial maps of AMSR-E, CLSM-OL, and CLSM-DA hydrologic extremes (surplus/deficit) for the May 2011 Midwest flood and December 2007 Southeastern drought. Table 1 provides goodness-of-fit statistics between AMSR-E and CLSM, including: adjusted-R^2, mean absolute error, Nash-Sutcliffe efficiency, and the index of agreement [*Willmott*, 1981].

All regions, except for the Southwest, were statistically significant at the 95% significance level. Even though the correlation between CLSM and AMSR-E is small in some areas, every statistic did show improvement in every region after model data assimilation. R^2 coefficients between AMSR-E/CLSM-OL ranged from 0.10 to 0.53 while AMSR-E/CLSM-DA coefficients ranged from 0.15 to 0.54. The highest correlations were found in the Northern Plains and Southwest. The CLSM performed the worst in the Southern Plains though assimilation improved the correlation by 10%. The smallest improvement was in the Southeast, where R^2 improved by a modest 1%.

Monthly, regional average TWSA from GRACE observations (black), CLSM-OL (purple), and CLSM-DA (green) are compared in Figure 6, starting in January 2013 and ending in April 2014. The last assimilation month is December 2013. During this period, CLSM-OL follows a similar pattern with GRACE, though TWSA values are too low, with the exception of months after September 2013 in the Northern and Southern Plains and Southwest, where TWSA is too high. When the green line is either in between the black and purple lines or close to the black line, the assimilation has improved the modeled TWSA value towards the observation. This can make a substantial difference when evaluating the occurrence and severity of flood and drought.

CLSM-DA is nearly an identical match with GRACE in June and December 2013 for the Southeast, February and June 2013 for the Northern Plains, July and December 2013 for the Southern Plains, and February 2013 for the Southwest. In these months, the CLSM-OL value was also closer to matching the GRACE observation compared to other months in the time series, so there was less for the assimilation to adjust. In the Southwest and Southern Plains, GRACE TWSA showed a large decrease in the summer yet both the CLSM-DA and CLSM-OL

39

failed to capture the fall. In all regions, the December assimilation improved the CLSM storage. Following the December assimilation, CLSM-DA matches the shape of the CLSM-OL time series except for the Northern Plains where CLSM-OL continues to increase while CLSM-DA levels off after February 2014.

3.5 Discussion

A comparison of hydrologic variables from direct observation, CLSM data-assimilated outputs, and CLSM Open-loop runs was conducted to evaluate the accuracy and utilization of CLSM-DA for hydrologic extremes analysis. Data assimilation provides temporal and spatial resolutions currently unattainable with GRACE alone. Correlation results show that data assimilation improved CLSM TWSA in all study regions. We conclude that CLSM-DA is a viable dataset for the monitoring of terrestrial hydrology and hydrologic analyses based on several benefits assimilation warrants. What have we gained from this analysis is another tool for flood and drought monitoring – one that identifies and quantifies terrestrial water storage extremes with higher resolution (compared with GRACE satellites), separation of terrestrial storage components, and near-real time data access.

Maps of individual extreme events reveal GRACE's ability to capture extreme events but the lack of resolution makes it inapplicable for more localized water resource management, who may need to determine the propagation of extremes as they cross countries and state lines. There was no distinctive succession of extremes with GRACE. CLSM-DA maps not only allow us to identify key areas being affected by flood or drought conditions, but maps of preceding months or seasons can help identify antecedent conditions that can lead to devastating circumstances in subsequent periods.

Multiple instances of over- or underestimation of surplus and deficits by CLSM-DA speaks to the model's inability to simulate accurate amplitudes of the annual (seasonal) cycle. This inconsistency translated through to the identification hydrologic extremes, producing multiple discrepancies between the timing and severity of surplus and deficit periods. The addition of *in situ* observations from groundwater wells, snowpack, and streamflow gauges can help improve the timing and amplitude of CLSM climatology, ultimately leading to more true to life simulations of present-day and impending terrestrial hydrologic extremes.

With vertical disaggregation from the CLSM, we were able to assess relationships between SWE, SFMC, RZMC and groundwater. Throughout the time series, GRACE-identified extremes persist several months after those identified by the CLSM-DA, indicating that there may be some system memory the model is not able to replicate, even with assimilation. There is also evidence of one-to-two month lags between deficit appearance in SFMC and RZMC and the groundwater layer, as water takes time to percolate down through the subsurface. This timing could be further influenced by human alterations to surface water and groundwater extraction for agricultural applications.

Data assimilation improved CLSM SFMC correlations with AMSR-E surface moisture observations in all four NCA zones to varying degrees. The Northern Plains and Southeast showed the smallest improvement after assimilation while the Southern Plains showed the greatest improvement. Discrepancies can be attributed to a mismatch of spatial and temporal characteristics of the CLSM and AMSR-E satellite observations [Figure 5] as well as shortcomings in AMSR-E retrieval algorithms. Specifically, vegetation and soil parameters are poorly known but greatly affect absolute moisture values. In a comparison of AMSR-E, the Scanning Multichannel Microwave Radiometer (SMMR), and modeled soil moisture from

41

CLSM, *Reichle et al.* (2007) state that AMSR-E retrievals tend to be considerably drier (low levels of absolute soil moisture) and show far less temporal variability (small dynamic range) compared with SMMR. Additionally, the skill of AMSR-E is modest to begin with and is lower than that of the CLSM; hence, correlation will be modest at best.

Measures of RMSE indicate that CLSM-OL does not possess enough information about the hydrologic system to produce an accurate estimate or depiction of TWSA compared with the CLSM-DA. Storage observed by GRACE versus the CLSM includes more terrestrial features, such as surface reservoirs, stream flow, human impacts on the hydrologic system (*e.g.*, dams, river divergences), and subsurface variations below the model's maximum depth (*i.e.*, below 2 meters). Assimilation corrects the CLSM towards GRACE but still does not address the inherent lack of physical properties in the terrestrial system. This is apparent in months following the last GRACE assimilation, where the CLSM-DA merely continues to follow the original CLSM-OL pattern.

Though improvements were often modest, I have shown the CLSM-DA to be superior to those from the CLSM-OL. Data assimilation in step in the right direction towards developing techniques that take full advantage of GRACE satellite observations and negate some of GRACE's shortcomings. Further model parameterization and integration of both *in situ* and remotely sensed observations (*e.g.*, groundwater wells, the Soil Moisture and Ocean Salinity (SMOS), Soil Moisture Active-Passive (SMAP) and GRACE-II missions) will continue to amend and improve the CLSM simulations, which will ultimately strengthen contributions to drought characterization and monitoring.

3.6 Acknowledgements

	Southeast	Northern Plains	Southern Plains	Southwest
AMSR-E / CLSM-OL				
Adjusted R-Squared	0.22	0.53	0.10	0.49
MAE	0.7617	0.4585	0.849	0.5872
SDR	0.9181	0.5788	1.0387	0.676
Nash-Sutcliffe	-0.4125	0.4168	-0.4591	0.3691
Index of Agreement	0.684	0.8506	0.5855	0.827
AMSR-E / CLSM-DA				
Adjusted R-Squared	0.23	0.56	0.20	0.56
MAE	0.6854	0.4541	0.8282	0.5701
SDR	0.8149	0.5784	0.9918	0.6609
Nash-Sutcliffe	-0.1104	0.4264	-0.3429	0.4095
Index of Agreement	0.7455	0.857	0.6189	0.8458

Table 3.1. Table of "Goodness-of-Fit" statistics for surface soil moisture content from AMSR-E, CLSM-OL, and CLSM-DA for NCA regions: Southwest, Northern Plains, Southern Plains, and Southeast. All statistics are significant at the 95% confidence level with the exception of the Southwest region. Though modest, all statistics improve with data assimilation.
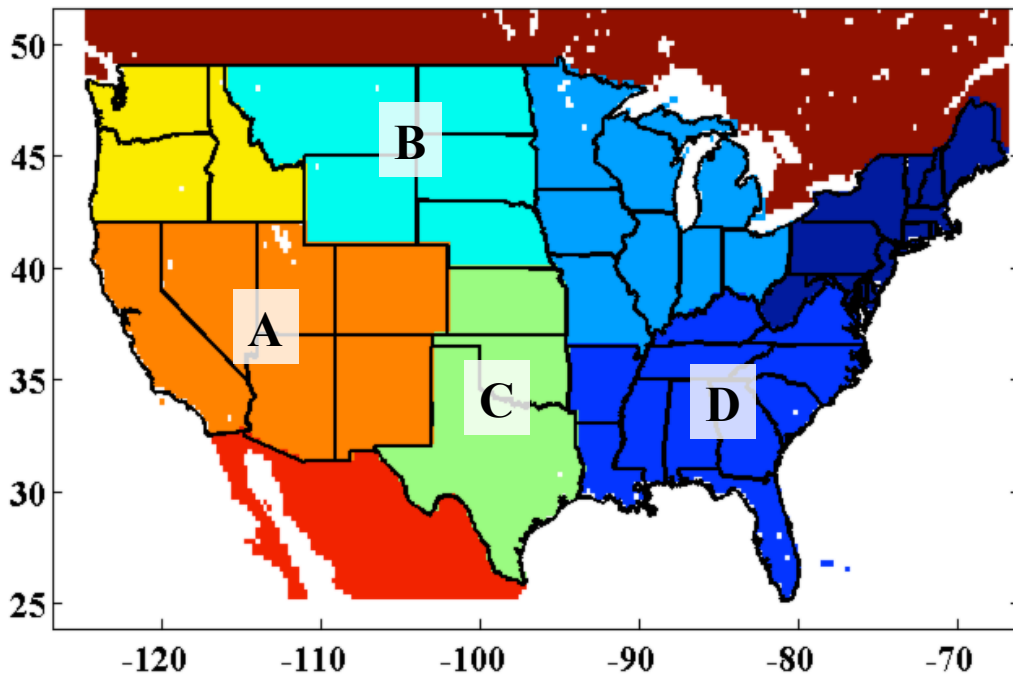
Figure 3.1. Map of National Climate Assessment (NCA) designated climate zones: (A) Southwest, (B) Northern Plains, (C) Southern Plains, and (D) Southeast. Region masks are used to produce monthly average time series of CLSM-DA outputs.
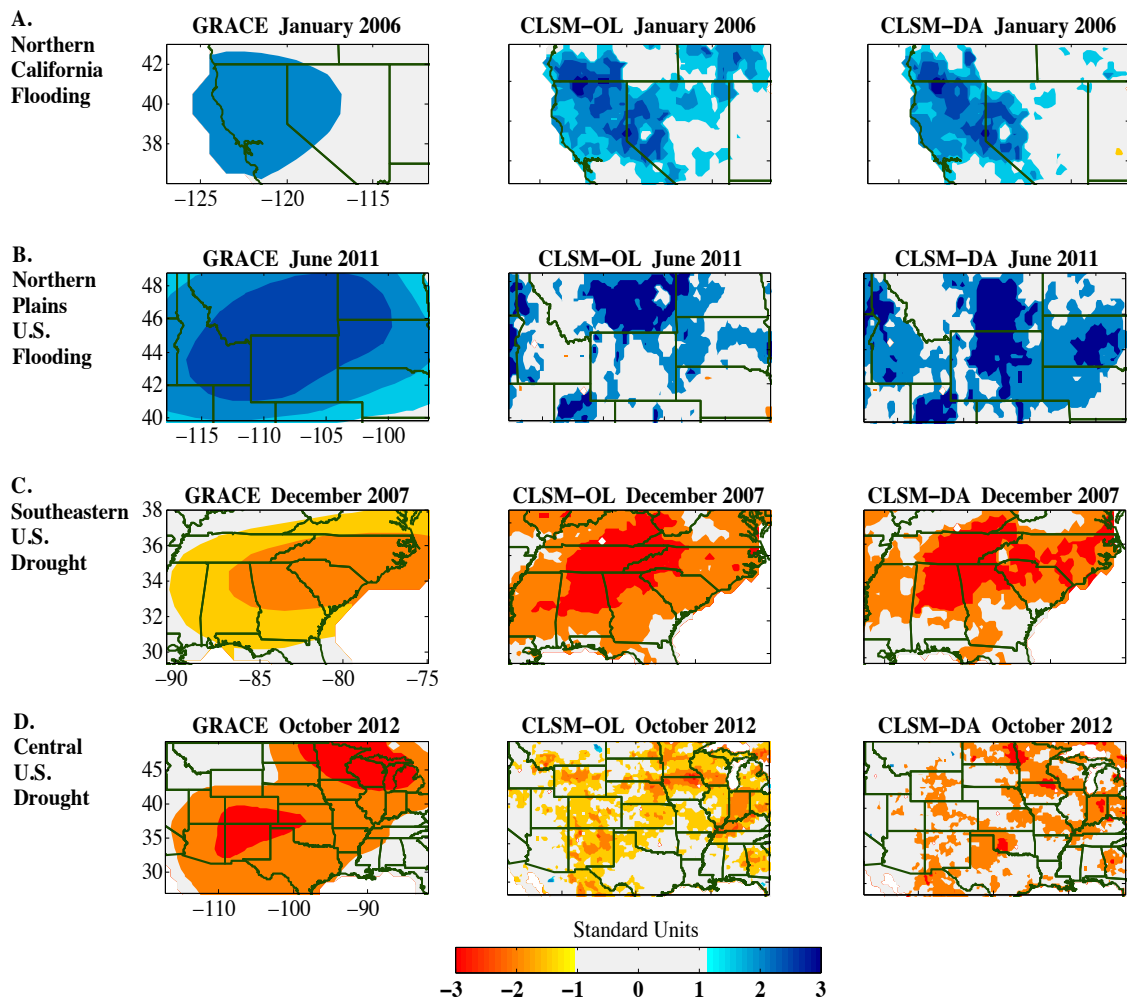
Figure 3.2. Spatial maps comparing two flood and two drought events in the United States during the GRACE period of record: (A) Northern California floods, (B) Northern Plains floods, (C) Southeastern drought, and (D) Central U.S. drought. *Left panels*, GRACE TWSA on one-degree grid. *Middle panels*, CLSM-OPENLOOP TWSA on quarter degree grid. *Right panels*, CLSM-DA TWSA on quarter degree grid. Data shown are residual TWSA, which represent surplus (blue) and deficit (red) water storage.
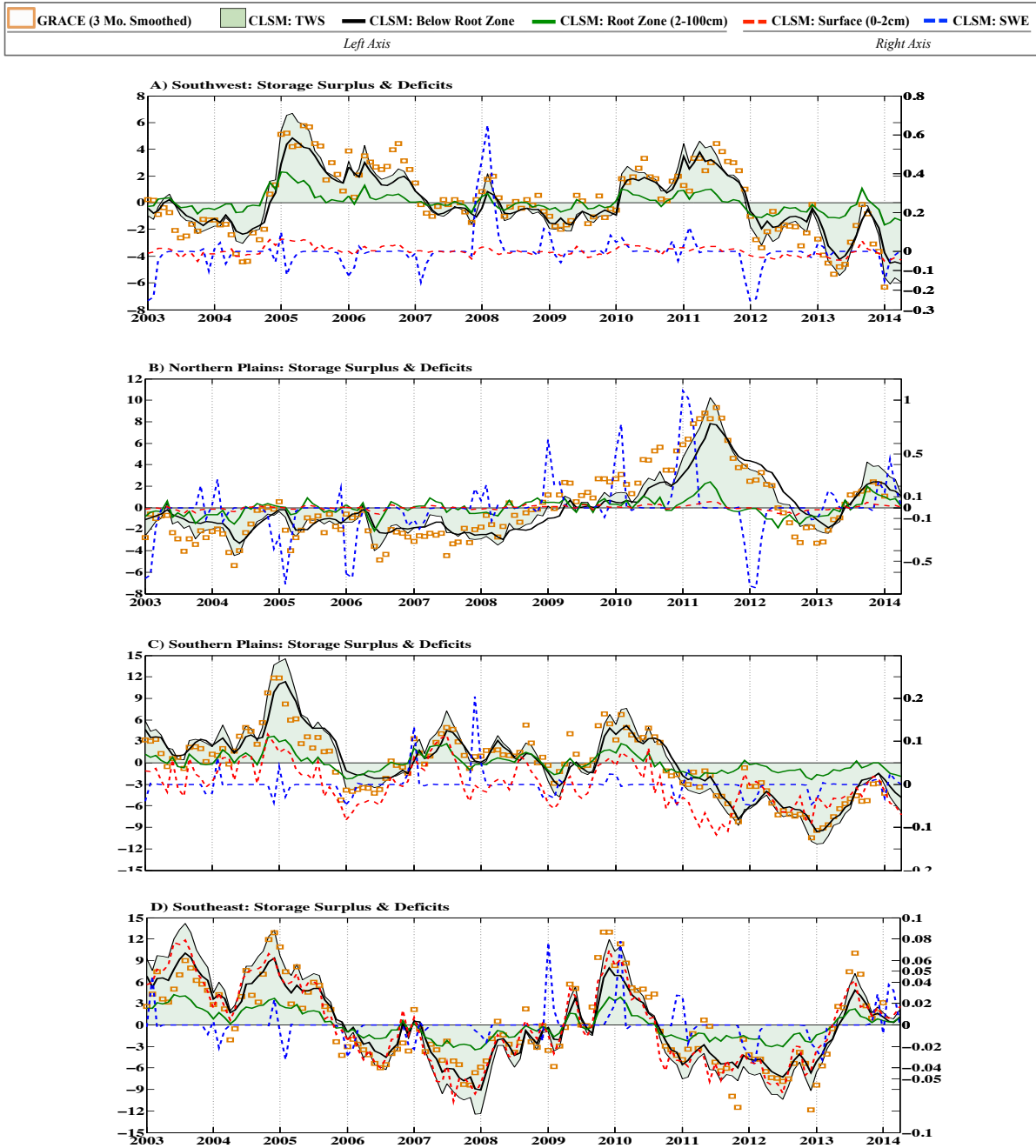
Figure 3.3. CLSM-DA disaggregated, residual terrestrial water storage time series for the four NCA regions: (A) Southwest, (B) Northern Plains, (C) Southern Plains, and (D) Southeast. Time period is from January 2003-April 2014. Negative values designate deficits and positive surplus. Variables on the left axis are: CLSM-DA total water storage (green shading), Below RZMC (black), RZMC (green), and monthly GRACE TWSA (gold squares). Variables on the right axis are: CLSM-DA SFMC (red dashed) and SWE (blue dashed). Units are centimeters of equivalent water storage.
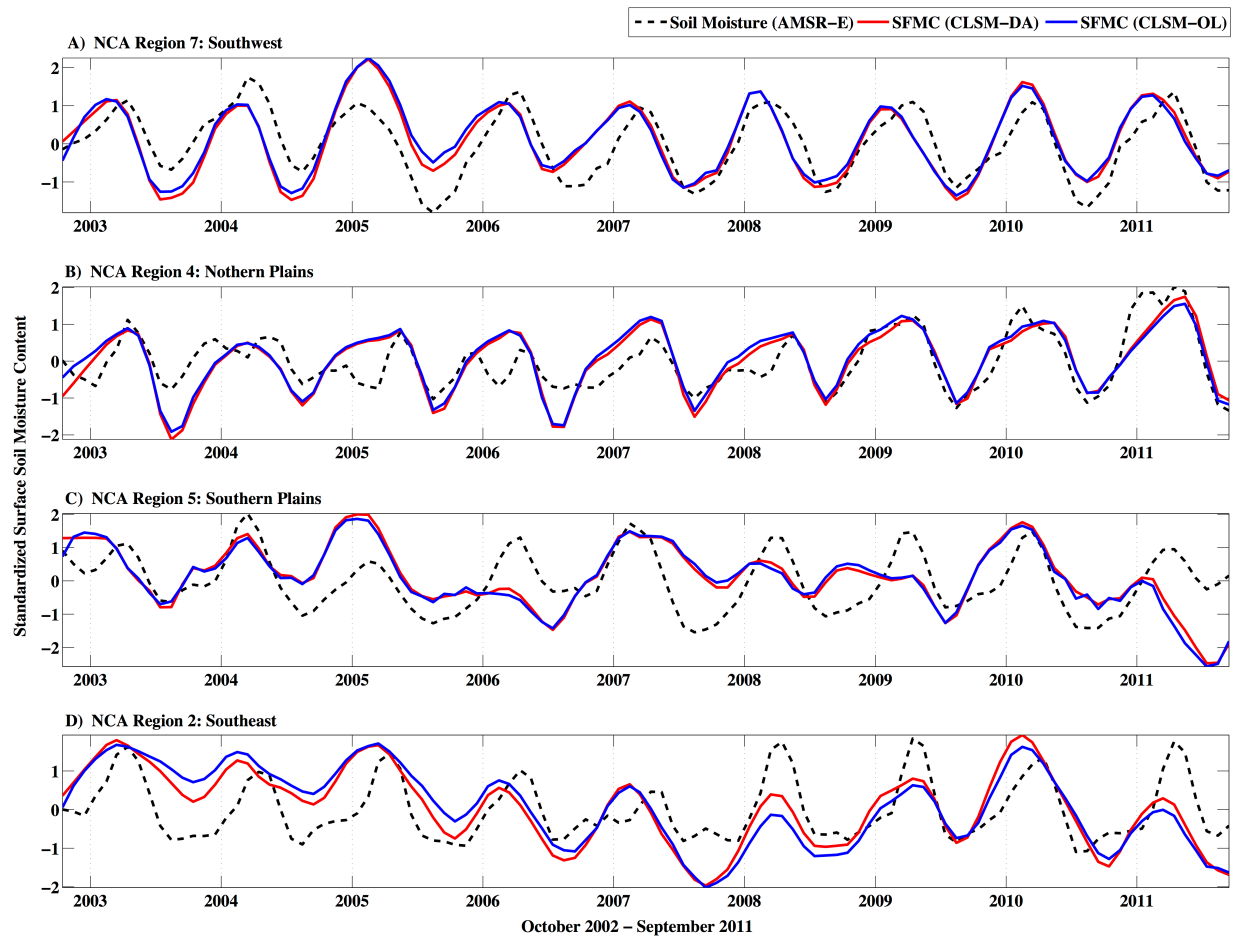
Figure 3.4. Comparison of CLSM-DA SFMC (red solid), CLSM-OPENLOOP SFMC (blue solid) and AMSR-E surface soil moisture (black dashed) for the four NCA regions: (A) Southwest, (B) Northern Plains, (C) Southern Plains, and (D) Southeast. Data are presented in standard units and a 4-month low pass filter was applied to smooth the time series. Time period is from October 2002-September 2011.
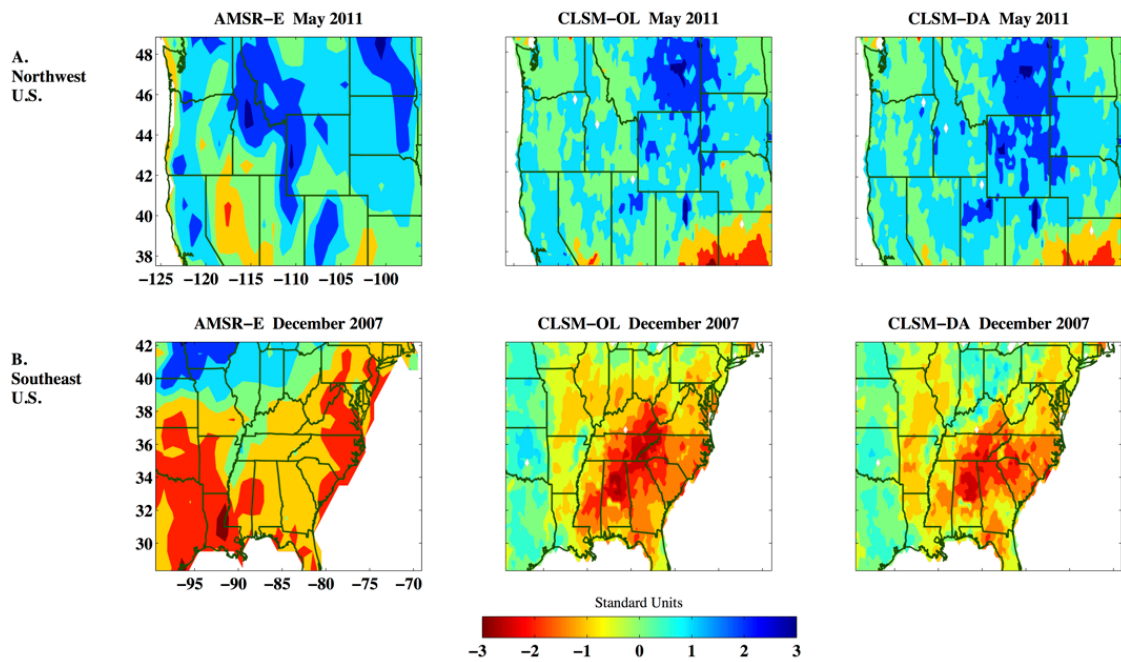
Figure 3.5. Spatial maps comparing AMSR-E surface soil moisture content and SFMC (0-2 cm layer) from CLSM-OL and CLSM-DA: (A) Northwestern U.S. and (B) Southeastern U.S. *Left panels*, AMSR-E soil moisture on one-degree grid. *Middle panels*, CLSM-OPENLOOP SFMC on quarter degree grid. *Right panels*, CLSM-DA SFMC on quarter degree grid. Data are shown in standard units.
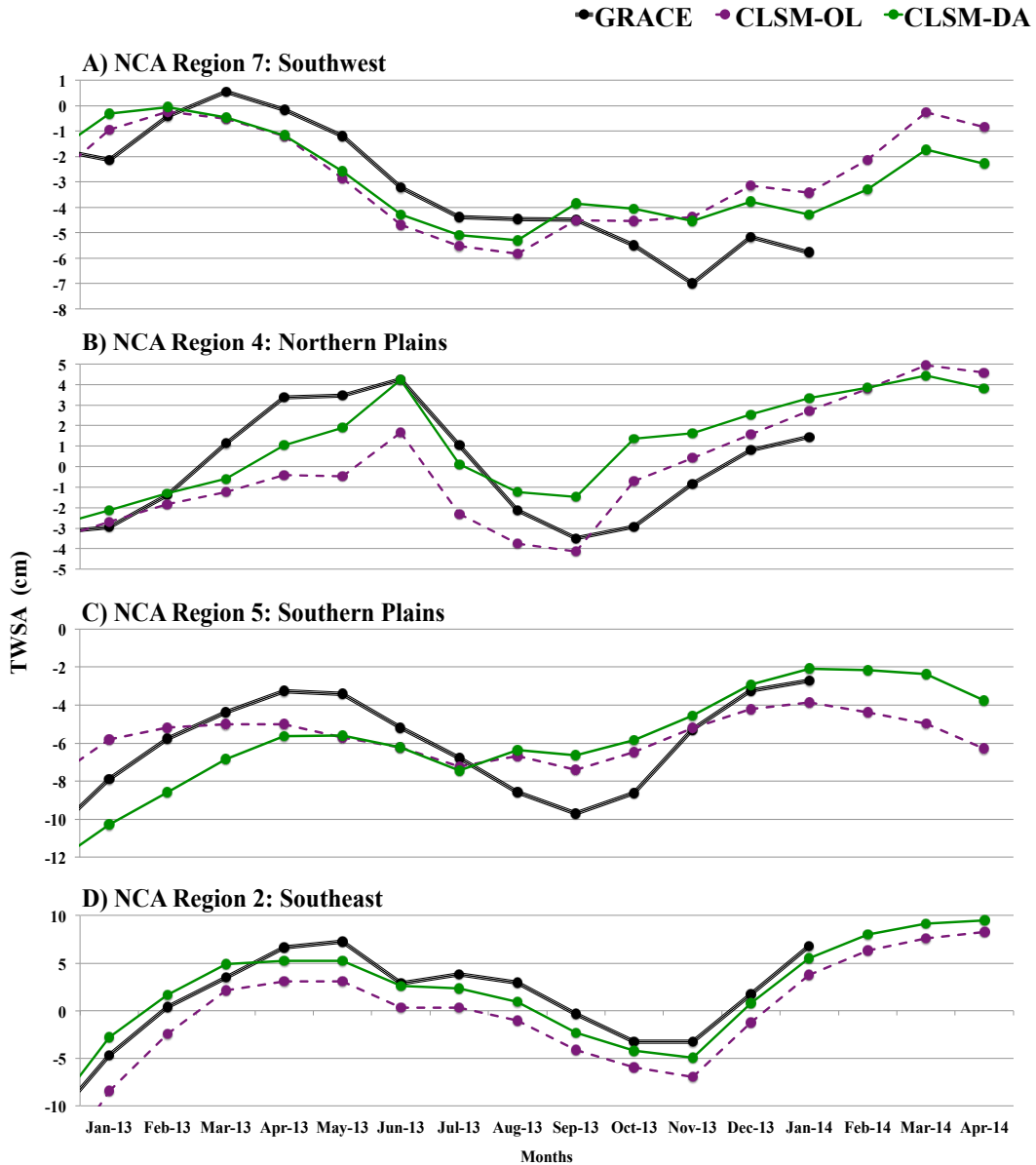
Figure 3.6. CLSM-DA degradation assessment: January 2013 to April 2014 time series of GRACE, CLSM-DA, and CLSM-OPENLOOP TWSA (cm) for the four NCA zones. Focus is on the last three months, after the last assimilation (December 2013). The CLSM time series (green) continued to run for February, March and April 2014 without assimilation with GRACE data (black double line). CLSM-OPENLOOP TWSA (purple) is also shown. NCA regions: (A) Southwest, (B) Northern Plains, (C) Southern Plains, and (D) Southeast.

50

Chapter 4

Evaluating the current (2014) hydrologic drought in California's Central Valley by extending GRACE storage anomalies via a multivariate, multi-frequency regression model

4.1 Introduction

California's Central Valley comprises the Sacramento, San Joaquin, and Tulare river basins and has been overwhelmed by drought conditions for more than three years, with no signs of recovering in the immediate future. Rain- and snowfall deficiencies combined with population growth, growing water demands in urban, agricultural and industrial sectors, in addition to unsustainable water use practices in agricultural and urban sectors have placed tremendous strain on the hydrologic system [*Gleick et al.*, 2014]. 100% of California has been in Moderate to Exceptional drought conditions since March 2014. Between April and June 2014, Exceptional drought conditions increased from 25% of the state to 34% [*U.S. Drought Monitor*, 2014]. With drier conditions expected to continue through the summer months, there is pressing need for hydrologic analysis concentrated on the Central Valley's terrestrial water storage (TWS) supply for the improved management of dwindling water resources.

The objective of this body of work is to extend GRACE TWS anomalies into the past, to compare the current drought with historic events, and into the future, to measure water deficiencies in California's Central Valley past the currently-available GRACE observation. This is accomplished by way of a multivariate, multi-frequency, linear regression model, which relates the annual and inter-annual frequencies of precipitation, evapotranspiration, and water storage data. With this synthetic storage record, we provide specific information about

51

hydrologic extremes (surplus and deficits) in California's Central Valley by utilizing the GRACE-based drought severity metric detailed in *Thomas et al.* [2014].

4.2 Data & Methods

4.2.1 Precipitation Data

Rainfall data used as input for the multi-frequency regression model was obtained from the PRISM Climate Group [*http://prism.oregonstate.edu*]. The PRISM dataset contains spatially gridded, monthly-average precipitation at 4 km grid cell resolution and covers the conterminous United States, starting in January 2002 and ending in June 2014. PRISM is an analytical model that uses point data and an underlying grid, such as a digital elevation model, to generate gridded estimates of monthly precipitation and temperature [refer to *Daly et al.*, 2008 for further details about methodology]. The PRISM dataset was chosen as the superior precipitation product for our regression model because it incorporates a conceptual framework that addresses the spatial scale and pattern of orographic processes, making it well suited to areas with mountainous terrain [*Daly et al.*, 2008]. The Sierra Nevada Range flanks the eastern boundary of the Central Valley region in this study; thus, the use of PRISM is considered optimal for capturing the spatial distribution of precipitation in the region. The most accurate precipitation available is essential for model development. We calculate the spatial average precipitation for each month within the Central Valley region and convert from mm to km^3 per month by multiplying by the basin area $(182,600 \ km^2)$.

The first step in preparing PRISM data for the regression model is to integrate through the time period by computing the cumulative sum throughout the time series. Integrating transforms the data to the cumulative sum of precipitation so that monthly water storage does not

have a time lag with rainfall. The mean is then removed to produce cumulative precipitation anomalies centered on zero. Lastly, we calculate a monthly climatology time series, which represents the annual (seasonal) precipitation frequency. This climatology is subtracted from the cumulative precipitation anomalies to represent the inter-annual (residual) precipitation cycles.

The National Oceanic and Atmospheric Administration (NOAA) Precipitation Over Land (PREC/L) dataset was used for two purposes: to utilize an alternative precipitation dataset other than the one used for model development and to estimate TWSA back in time through 1948. The use of this model need not be constrained to one specific precipitation dataset. NOAA/OAR/ESRL PSD houses the PREC/L dataset [*http://www.esrl.noaa.gov/psd/*]. The record contains monthly averaged, surface-level precipitation totals in units of millimeters per day. The mean distribution and annual cycle of precipitation observed in PREC/L showed good agreement with those in several published gauge-based datasets, and the anomaly patterns associated with ENSO resemble those found in previous studies [*Chen et al.,* 2002]. Data are posted on one-degree global grids for a time period from January 1948 to June 2014. We convert the data from mm to km^3 per month and spatially average for the Central Valley region.

4.2.2 Evapotranspiration Data

Total, monthly-average evapotranspiration (ET) data were obtained from the National Centers for Environmental Prediction/Oregon State University/Air Force/Hydrologic Research Lab (Noah) land surface model for Version 2 of the Global Land Data Assimilation System (GLDAS-2; *Rodell et al.*, 2004). The Noah model [*Ek et al.*, 2003] is a stand-alone, 1-D column model designed to mathematically and numerically represent land surface characteristics (land cover), states (temperature, snow, and soil moisture), and fluxes (total evapotranspiration,

photosynthesis, and radiation) as a function of both space and time. The model applies finite-difference spatial discretization methods and a Crank-Nicholson time-integration scheme to numerically integrate the governing equations of the physical processes of the soil-vegetation-snowpack medium [*Ek et al.*, 2003].

Noah has 33 parameters: 10 related to vegetation and 23 that describe soil properties with a four soil layer structure: 10-cm top layer, root zone layer of 20 cm, deep root zone of 60 cm, and a sub-root zone of 110 cm. Simulations are forced by the global meteorological forcing dataset from Princeton University [*Sheffield et al.*, 2006]. The model was initialized on January 1, 1948 using soil moisture and other state fields. The total evapotranspiration dataset is posted on a global, quarter-degree grid with temporal coverage from January 1948 to June 2014.

Modeled total evapotranspiration data were chosen for their temporal and spatial coverage. Simulations of water store change also compare well with GRACE observations [*Yang et al.*, 2011]. Data were downloaded from the Goddard Earth Sciences Data and Information Services Center (GES DISC). Total ET values were converted from $kg/m^2/s$ to km^3 per month and spatially averaged for the Central Valley region. ET data are prepared for the regression model by removing the long-term mean to produce monthly anomalies. Similar to the precipitation dataset, we calculate both monthly climatology and residual ET anomaly time series, to represent annual (seasonal) and inter-annual (residual) ET cycles.

4.2.3 GRACE Data

The GRACE dataset is a monthly, global, one-degree gridded, scaled GRACE land data product, processed by the Texas Center for Space Research [CSR; version CSR-RL05]). The time period is from April 2002 to April 2014. A basin mask for the Central Valley [Figure 1] was

used to calculate monthly, spatially averaged terrestrial water storage anomalies (TWSA). Central Valley regional-average anomalies were then multiplied by the region's area to produce regional-average water storage volume anomalies in units of km^3. Total regional average error, which accounts for measurement and leakage errors, is 33.2 mm (6.06 km^3). Refer to *Swenson and Wahr* [2006] and *Wahr et al.* [1998] for post-processing details and to *Landerer and Swenson* [2012] for particulars on signal restoration, scaling, and regional error calculation.

4.2.4 PHDI and SPI Drought Indices

Two of the more widely used drought indices, the Palmer Hydrological Drought Index (PHDI) and one-month Standardized Precipitation Index (SPI), were chosen to compare with model estimates of historic water storage extremes. Water resource managers commonly use these indices for assessments of drought severity and planning strategies. The PHDI is an adjustment to Palmer's Drought Severity Index (PDSI) [*Palmer*, 1965], which characterizes the severity of dry and wet periods over the United States based on monthly temperature and precipitation data in addition to the soil-water holding capacity at a specified location. In near-real time, PDSI is no longer a meteorological index but becomes a hydrological index (PHDI) because it is based on moisture inflow (precipitation), outflow, and storage, and does not take into account the long-term trend [*Karl and Knight*, 1985]. PDSI and PHDI are identical during an established spell but differ during the onset and ending of a spell. The PHDI uses the Penman-Monteith method for estimating potential evaporation with a record covering January 1948-December 2012.

The SPI was developed by *McKee et al.* [1993] and represents the number of standard deviations that observed cumulative precipitation deviates from the climatological average. The

index is based entirely on monthly precipitation accumulations using the PREC/L precipitation dataset. The methodology is based on a Pearson Type III (*i.e.*, 3-parameter gamma) distribution as suggested by *Guttman* [1999] and describes standard deviations from the long-term average (30+ years). PHSI and SPI values are interpolated to one-degree grids (using a 2-D, nearest neighbor interpolation scheme), spatially averaged for the Central Valley region, and presented in standardized units of relative wet and dry conditions. The SPI record extends from January 1948-May 2014

4.2.5 Multivariate, Multi-Frequency Regression Model

A conceptual schematic of the multivariate, multi-frequency regression model is provided in Figure 2. The basis of this model builds on the concept of a water balance throughout the three watersheds in the Central Valley region, where changes in storage result from inputs of precipitation and outputs of runoff and ET over time (see Equation 4.1). The proposed model provides a measure of the expected amount of change in monthly water storage the Central Valley can expect to receive from a certain amount of precipitation and ET, which can be updated as additional monthly data becomes available.

$$\frac{d\mathrm{S}}{dt} = \mathrm{P} - \mathrm{ET} - \mathrm{R} \;\; \rightarrow \;\; d\mathrm{S} = (\mathrm{P} - \mathrm{ET} - \mathrm{R})dt$$

(Equation 4.1);

where changes in water storage (dS) are equal to variations in precipitation (P), evapotranspiration (ET), and runoff (R) over time (dt).

For my regression model, I concentrated on the two atmospheric fluxes in the water balance equation (*e.g.*, P and ET). Precipitation is the natural input into the system while ET is

additionally influenced by anthropogenic activities (*i.e.*, reservoir management, irrigation, and water diversion). Rearranging Eq. 4.1 and representing error terms as $\varepsilon dt = R + e$ (*e* includes model error in addition to errors associated with the omission of runoff) results in the following equation:

$$dS - Pdt + ETdt = \varepsilon dt$$

(Equation 4.2);

I then parameterize the runoff term as a linear function of P and ET (*e.g.*, $R = \beta_1 P + \beta_2 ET$) to create a linear, multivariate regression model, which takes the following form:

$$dS = \beta_1 P + \beta_2 ET \pm e$$

(Equation 4.3);

where the response variable is water storage change (dS), predictor variables are integrated precipitation (P) and evapotranspiration anomalies (ET), regression coefficients are represented by β, and *e* is the error term. All parameters are time-variant.

The model utilizes a dynamic regression approach, identifying relationships between precipitation, evapotranspiration, and water storage anomalies based on their annual and inter-annual frequencies (cycles). I split the time series into these components because I wanted to account for response differences between variables at different timescale. For example, on annual and inter-annual scales, P varies mainly in response to climatic variations, while ET and R respond differently depending on climate as well as water management activities within the region. This is particularly important for the heavily managed Central Valley.

By independently inputting these frequencies into the regression model, I can represent the characteristics of each, which have varied impacts on hydrologic extremes [*Billah and Goodall*, 2011; *Jongen et al.*, 2011]. The annual cycle is driven by seasonal variations in climate, recognized by its sinusoidal waveform. The inter-annual cycle is a residual of the annual where variations are often associated with inter-annual oscillations such as ENSO and NAO [*Meehl*, 1987]. Figure 3 shows time series of this separation of annual (Figure 3b) and inter-annual (Figure 3c) frequencies for integrated PRISM precipitation anomalies (blue), Noah evapotranspiration anomalies (green), and GRACE TWSA (black), in addition to the original datasets (Figure 3a).

The annual and inter-annual modes for TWSA, precipitation, and evapotranspiration time series are individually entered into a regression equation (Eq. 4.3) to estimate the contribution of each frequency to its associated storage signal. The model produces regression coefficients for the annual (β_1) and inter-annual (β_2) modes, which represent a parameterization for the omitted runoff variable. Coefficients are subsequently multiplied with frequency-specific precipitation and evapotranspiration data to estimate TWSA. New precipitation and ET datasets must be prepared as was detailed in Sections 4.2.1 and 4.2.2, before multiplying with their respective regression coefficients. The final step is to sum the annual and inter-annual TWSA estimates to construct final, synthetic total water storage anomalies.

Model residuals were tested to assure that they fit the assumptions of an ordinary least squares regression analysis (i.e., normally distributed, heteroscedastic, and uncorrelated). Annual and inter-annual residuals displayed normal distributions. A Breusch-Pagan test for conditional heteroscedasticity [*Breusch and Pagan*, 1979] revealed that heteroscedasticity was not a multiplicative function of the predicted values. Durbin-Watson (dw) tests for autocorrelation

[*Durbin and Watson*, 1950] indicated that inter-annual residuals were positively correlated (dw: 0.609) and annual residuals were uncorrelated (dw: 1.819). To address correlation and quantify the reliability of the model, I ran a 14200-sample bootstrapping procedure to assess how model predictions of β_1 and β_2 changed as the data sample changed. Bootstrapping attained comparable regression coefficients even with different samples (β_1 values had a spread of 0.070 and β_2 values had a spread of 0.158), which leads me to conclude that I have developed a reliable model structure that is not undesirably affected by correlation of residuals in the inter-annual mode.

Coefficients of determination (adjusted-R^2), adjusted for the number of predictors in the model, are used to evaluate the correlation between modeled and observed TWSA. Standard error (in km^3) on each regression coefficient ($\beta_{1,2}$) is propagated through the analyses, multiplied by two, and is then shown as 95% confidence error bounds about the model estimated TWSA time series (e.g., 1.22 km^3). Root Mean Squared Error (RMSE) and the Index of Agreement [*Willmott*, 1981] are computed as a means to compare the accuracy of the regression-based storage estimates. RMSE represents the sample standard deviation of the differences between modeled and observed value. The Nash-Sutcliffe efficiency, F- and t-statistics are also provided in the evaluation of model accuracy.

4.3 Results

Table 1 lists results from the multivariate, multi-frequency regression model: the regression coefficient (*Estimate*), standard error of the estimate (*SE*), p-value for the *t*-statistic (*pValue*), the *t*-statistic (*t-Statistic*), and the *F*-statistic (*F-Statistic*) for the annual (Table 1a) and inter-annual (Table 1b) frequencies. Additional model statistics are: error degrees of freedom, RMSE, R^2, and adjusted R^2. Precipitation regression coefficients are 1.1749 for the annual mode

(β_1) and 0.2768 for the inter-annual mode (β_2). ET regression coefficients are -0.129 for the annual mode (β_1) and 3.06 for the inter-annual mode (β_2).

Standard errors on β_1 are 0.0195 and 0.0655 km^3 and β_2 are 0.0245 and 0.5016 km^3 for precipitation and ET, respectively. Combined error on the regression coefficient estimates is 1.22 km^3 (at the 95% confidence level). Annual and inter-annual model RMSE's are 2.11 and 8.43, respectively. Results from one-sample student's t-tests specify that inter-annual precipitation and evapotranspiration as well as annual precipitation results are significant at the 0.01 level, while annual evapotranspiration results are significant at the 0.05 level.

Figure 4a shows time series of GRACE with ± regional average error shading (6.06 km^3; blue) and modeled storage with ± error on the model coefficients (1.22 km^3; orange). A 3-month smoothing filter was applied to both time series. In Figure 4b, I ran the model with PRISM precipitation from April 2002-June 2014, a two-month extension of the current-most available GRACE observation. Model TWSA estimates are shown in orange, alongside GRACE TWSA (blue bars). Model TWSA gradually decreased in the months following GRACE observations through June 2014, which has a storage anomaly of -23.5 km^3. Figure 4c shows a scatter plot of GRACE and model storage to illustrate the spread of values between the time series. The adjusted-R^2 between GRACE TWSA and model estimates is 0.8237, the Nash-Sutcliffe efficiency is 0.8248, the index of agreement is 0.95, and the RMSE is 7.13.

Modeled storage overestimated the amplitude of peak negative anomalies at the end of 2005 by 13 km^3. Additionally, in 2007 and 2012, positive anomalies were overestimated by 11-12 km^3. The largest underestimation of positive storage (21 km^3) occurred in 2005. The model also underestimated negative storage at the end of 2007 by 10 km^3. The timing of anomalies is

comparable throughout the records though, in mid-2013, model anomalies begin to decline quicker than GRACE. Model discrepancies are further examined in the Discussion Section.

Figure 5a showcases hydrologic extremes (surplus and deficit) identified by the regression model (orange shading) and GRACE observations (blue bars). Figure 5b displays only present months from April 2013-June 2014. June 2014 displays an estimated water storage deficit of -28.8 km^3. Figure 5c and 5d show a scatter plot and annual TWSA monthly climatology for the two datasets. The regression model matched 60% of the hydrologic surplus/deficit occurrences identified by GRACE. The largest discrepancies were in 2005 and late 2008 through early 2009 where the model estimated surplus storage and GRACE observed deficits. This was the opposite case in late 2003 where the model continued to identify five months of storage deficits and GRACE observed recovery. The onset of extreme conditions from the model lag GRACE by 2-3 months in 2004 and 2014.

A time series of reconstructed, historic (*i.e.*, January 1948 to June 2014) water storage residuals (black) along with PHDI values (beige) and SPI values (light red) are show in Figure 6. I standardized the storage estimates by dividing each monthly value by the time series' standard deviation. Negative PHDI and SPI values represent dry months while positive values represent wet months. Similarly, negative storage represents a deficit and positive represents surplus. R^2 between estimated storage residuals and PHDI is 28% and 3% with 1-month SPI.

4.4 Discussion

A model has been proposed to relate precipitation and evapotranspiration to water storage anomalies in California's Central Valley based on a linear, multivariate, multi-frequency regression analysis. This work delivers a practical extension of research specifically related to

the use of GRACE TWSA observations for hydrologic extreme analyses. The main advantage is in the model's ability to estimate water storage changes beyond the last available GRACE observation (April 2014) and back in time to 1948 without the need for climate or land models. The model will continue to improve as more GRACE data become available.

The regression model explained 82% of GRACE's TWSA signal, under an assumption of linear relationships with rainfall and ET. The size of the coefficients for precipitation and ET tells us the magnitude of the effect each variable has on changes in water storage. For the annual mode, the model states that storage is predicted to increase 1.17 km^3 when precipitation increases one km^3 and to decrease by 0.13 km^3 when ET increases one unit. In the inter-annual mode, storage is predicted to increase by 0.28 and 3 km^3 when precipitation and ET increase one km^3, respectively.

The positive, inter-annual ET coefficient was unexpected because the water balance (Eq. 4.1) indicates that storage should decrease with increasing ET. One explanation for this could be groundwater extraction and irrigation throughout the Central Valley, which can interfere with linearity and conservation of mass within the system and affect the model's ability to represent relationships between the variables. The inter-annual ET coefficient had the largest deviation from one, which implies that the model has attempted to compensate for an underestimation of ET or it has attempted to account for errors resulting from the omission of runoff; a key component in the water balance equation.

Regression coefficients may also be compensating for correlation between P and ET, since all predictors in the model have influence on each coefficient. Multicollinearity may explain why coefficients deviate from one in the linear model. A Belsley test for multicollinearity [*Besley et al.*, 2004] produced variance inflation factors (VIF) of 2.2 for the

annual mode and 1.0 for the inter-annual mode. The VIF's specify that precipitation and ET are not correlated in the inter-annual mode, but multicollinearity is present in the annual mode. However, multicollinearity is not very high and should not adversely affect model significance.

Since the model only considers precipitation and evapotranspiration it is not able to explicitly account for deeper subsurface storage, which is a substantial component of the GRACE terrestrial water storage signal. This helps with explaining why the model underestimated several peak positive anomalies and overestimated a few months with higher negative anomalies. The capacity of the system to hold water lies in the variability of subsurface storage and snowpack, not just with rainfall and ET.

Further, anthropogenic impacts, which may weaken the correlation between groundwater level and rainfall, are not explicitly considered in this analysis. The response of each individual river basin in the Central Valley domain can be dominated by any combination of additional mechanisms including antecedent moisture conditions, varying magnitude of rain- and snowfall events, generation of runoff in different parts of the catchment, and heterogeneity in soil hydraulic properties [*Sophocleous*, 2002]. Moreover, GRACE observes changes in TWS resulting from both natural and anthropogenic factors. Surface reservoirs are heavily managed, so the addition of this variable to the model estimates would help account for seasonal-to-annual water storage changes that are not a direct result of precipitation variation.

With model estimates of water storage for the current-most month (June 2014) I determined that the Central Valley continued to face a deficit of approx. -29 km^3 of water, which was a key deliverable in the execution of this project. In the early part of the record as well as 2005, 2006, and 2014, modeled extremes lag GRACE observations by about 2 months (at the time of writing). The model also tends to stay wet for a longer period of time compared with

63

observations. These instances can be attributed to the model's TWSA climatology (Figure 5d), which are similar to GRACE except in April, May, and June where peak anomalies are overestimated. The climatology can be constrained by introducing subsurface well data into the model to help account for terms that exhibit variations on longer frequencies (*e.g.*, longer timescales for changes in groundwater to occur compared with surface moisture).

Comparisons of estimated hydrologic extremes with PHDI and SPI drought indices highlight what I expect to see from a GRACE-based drought measure, which is a metric that highlights terrestrial moisture states. Since SPI focuses on the meteorological form of drought it is not expected to match our water storage-based measure month-for-month, though it allows us to identify how meteorological drought affects changes in terrestrial storage. Moreover, in an assessment of long-term variations in PDSI (PHDI), *Sheffield et al.* [2012] state that this metric is oversensitive to changes in temperature, and other simplifications, which compromise its accuracy. Further inconsistencies suggest that precipitation and ET data are not sufficient enough, on their own, to assess all of the historic variations in extremes. This issue can be addressed with the addition of historic surface reservoir storage and groundwater well data that will provide more storage reservoir memory to the analysis, expectantly adjusting the timing and severity of hydrologic extremes.

Nevertheless, two major California droughts in 1976-77 and 1988-92 were clearly identified in the storage reconstruction, illustrating that more severe (larger magnitude) deficits may only manifest during the most severe meteorological drought episodes, as there is a larger system-wide impact from precipitation deficiencies. The current California drought so far has an average deficit of approx. -10 km^3 over 15 months. The 1990's and 1970's droughts average water storage deficits were 5-6 km^3 for episodes lasting 2-5 years, revealing that present

hydrologic conditions are undeniably more severe than California has faced in the past. With California entering into the dry season, there is little chance for recovery from natural sources; hence, activities such as improved efficiency, water use and reallocation, supply augmentation, funding adaptation, and stormwater capture will become progressively indispensable in the coming years [*Hanak and Lund*, 2012; *Gleick et al.*, 2014].

This work has merely scratched the surface of realizing the potential that exists in translating precipitation to terrestrial water storage and ultimately to available water resources, not only for California but worldwide. Further work is obligatory to test this regression model structure in river basins with different climatologic conditions (*e.g.*, regions with more diverse seasonality may have more complex relationships between rainfall, snow, and water storage in surface and subsurface layers). The statistical relationship between rainfall and water storage determined by our model can also be utilized in climate change studies to evaluate future water storage change under varying emissions scenarios. For example, using 50-to-100-year precipitation projections and modeled total ET as inputs into this type of regression-based model to estimate the associated water storage changes.

4.5 Acknowledgements

	A. Annual Regression Results:				B. Inter-Annual Regression Results:			
	Estimate	**SE**	**t-stat**	**pValue**	**Estimate**	**SE**	**t-stat**	**pValue**
Precipitation	*1.1749* *(± 0.0093)*	0.019541	60.12	2.13E-103	*0.2768* *(± 0.0029)*	0.024455	11.32	1.30E-21
Evapotranspiration	*-0.129* *(± 0.0311)*	0.065455	-1.97	0.05	*3.06* *(± 0.0595)*	0.50164	6.1	9.40E-09
	Model f-stat: 3779.6				Model f-stat: 101.4			
	Model Root Mean Squared Error: 2.11				Model Root Mean Squared Error: 8.43			
	Number of observations: 145, Error degrees of freedom: 143							

Table 4.1. Results of the P/ET/GRACE multivariate, multi-frequency regression model for (A) Annual and (B) Inter-Annual modes: the estimated coefficient value (Estimate) with error bars, standard error of the estimate (SE), t statistic (tStat), p-value for the t statistic (pValue), and the f-statistic (f-stat) for the annual (Table 1a) and inter-annual (Table 1b) modes. Additional model statistics are also provided: RMSE and error degrees of freedom. Inter-annual precipitation and evapotranspiration as well as annual precipitation results are significant at the 1% significance level. Annual evapotranspiration results are significant at the 5% significance level.
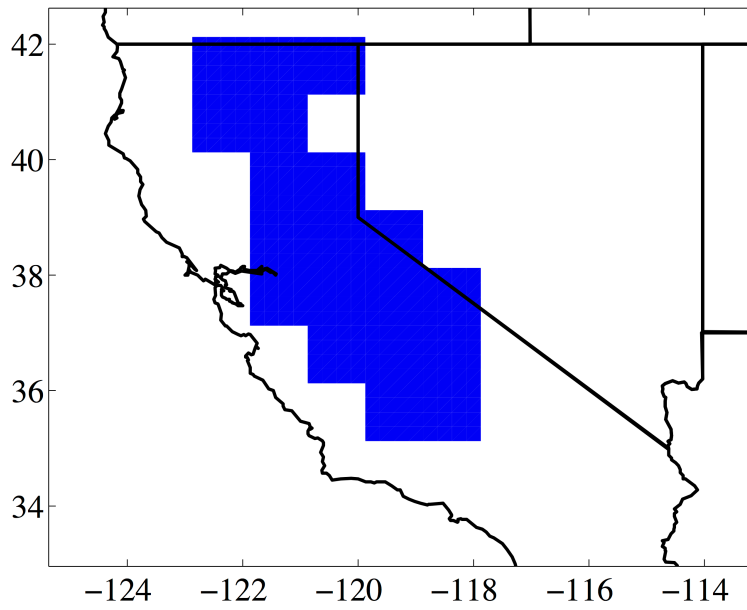
Figure 4.1. Map of the Central Valley study region. The region includes the Sacramento, San Joaquin, and Tulare watersheds and has an area of 182,598 km^2.
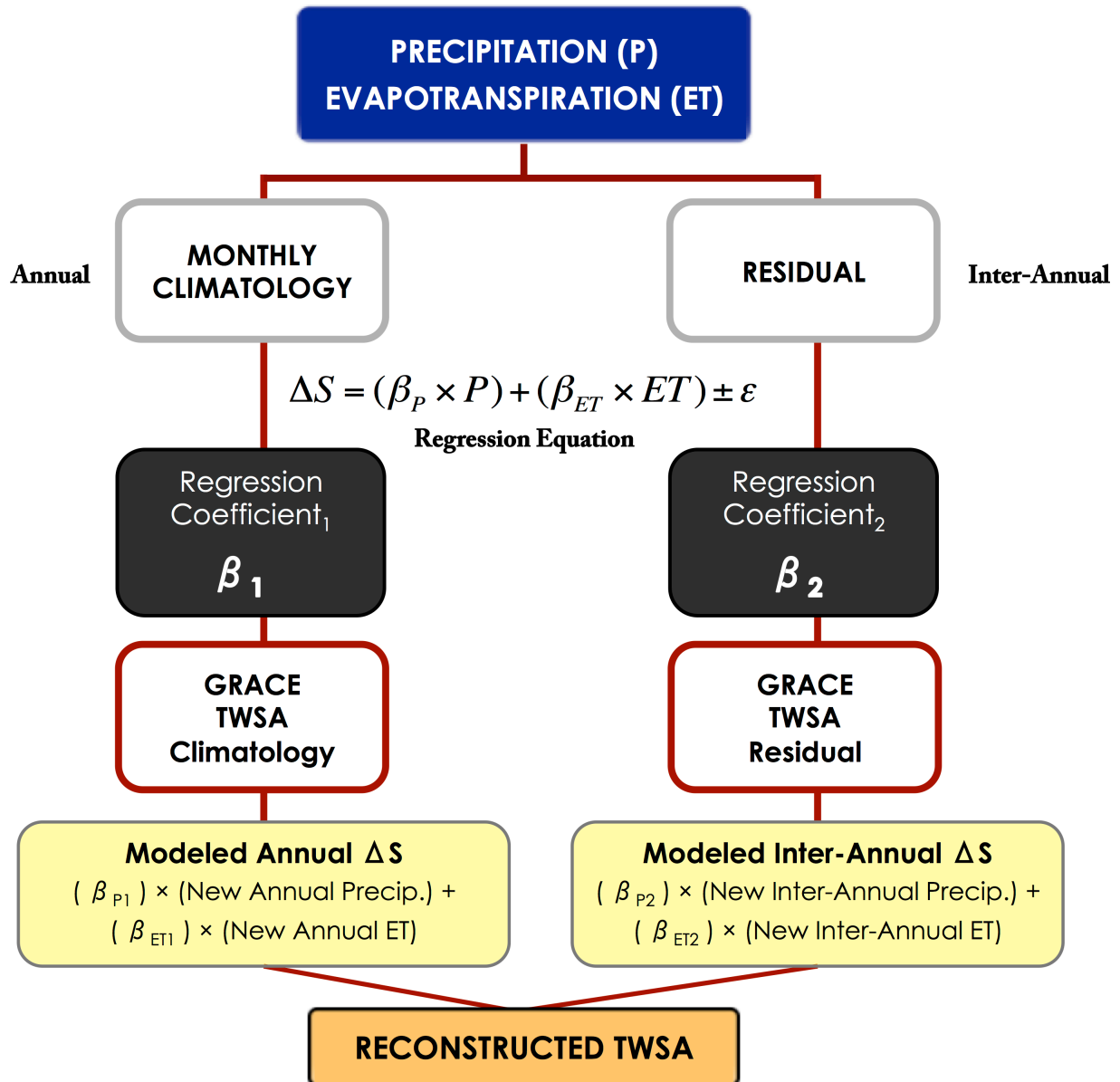
Figure 4.2. Conceptual schematic of the Multivariate, Multi-Frequency Regression Analysis: Precipitation data are de-trended, integrated, and then split into two frequencies, annual and inter-annual (residual). Evapotranspiration and GRACE data are also de-trended and split into annual and inter-annual time series. The time period used for regression analysis is April 2002- April 2014. The inter-annual frequency is calculated by removing the monthly climatology (annual frequency). The regression equation (shown in the middle) is used to calculate annual and inter-annual regression coefficients (β); where S is modeled, monthly TWSA, P is monthly PRISM precipitation, ET is monthly evapotranspiration from the GLDAS/Noah model, and ε are the errors (residuals). Units are cubic kilometers.
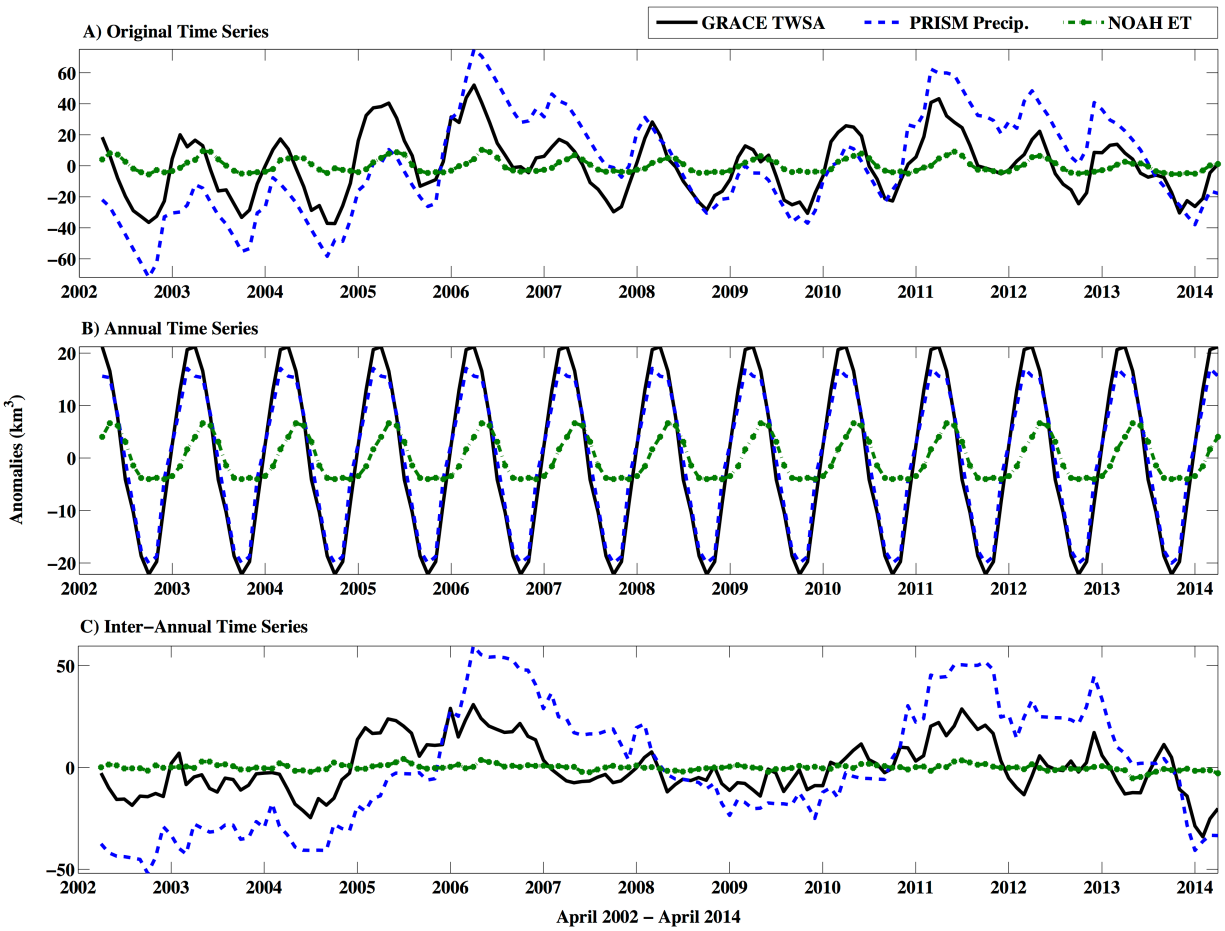
Figure 4.3. Time series of original (Figure 2a), annual (Figure 2b), and inter-annual (Figure 2c) precipitation (blue), evapotranspiration (green), and GRACE water storage (black) anomalies: April 2002 to April 2014. Inter-annual frequencies are calculated by subtracting the annual frequency from the precipitation anomalies. Units are cubic kilometers.
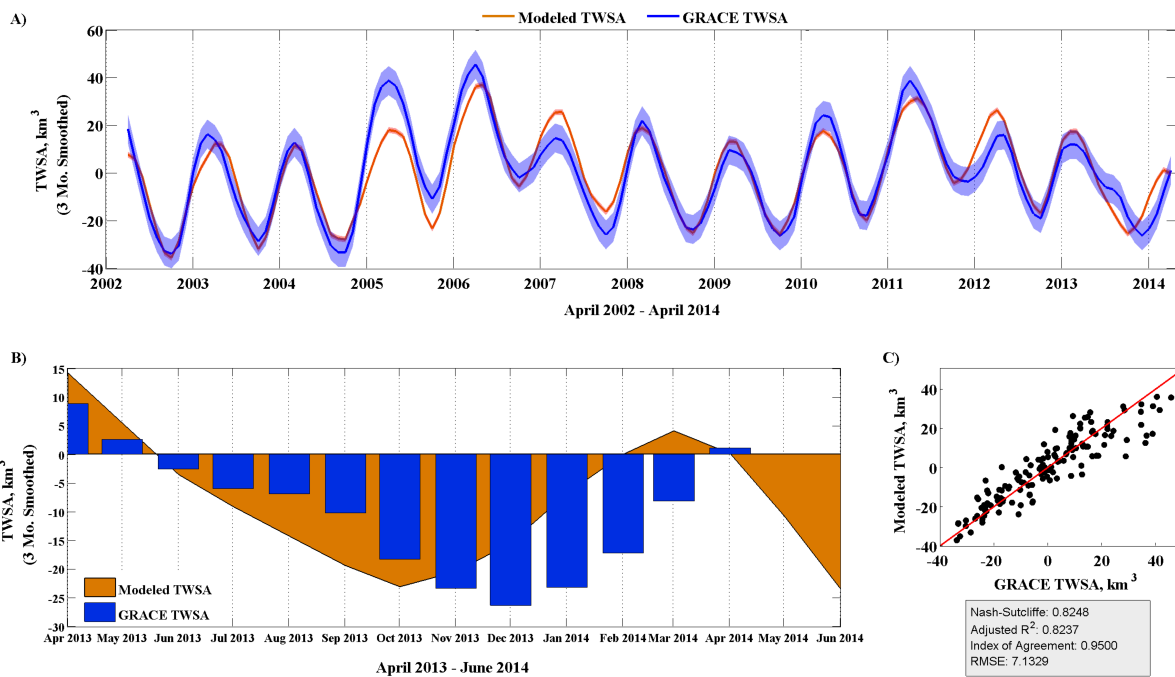
Figure 4.4. (A) Modeled storage (orange line ± error on regression coefficients {1.22 km^3}) and GRACE TWSA (blue line ± regional average error {6.06 km^3}) from April 2002-April 2014. (B) Two-month extension of estimated TWSA for the time period April 2002-June 2014. PRISM monthly, precipitation was used for this reconstruction. (C) Scatter plot of modeled and GRACE-observed TWSA with RMSE, Nash-Sutcliffe, and R^2. All time series have been smoothed with a 3-month low pass filter. Units are cubic kilometers.

70
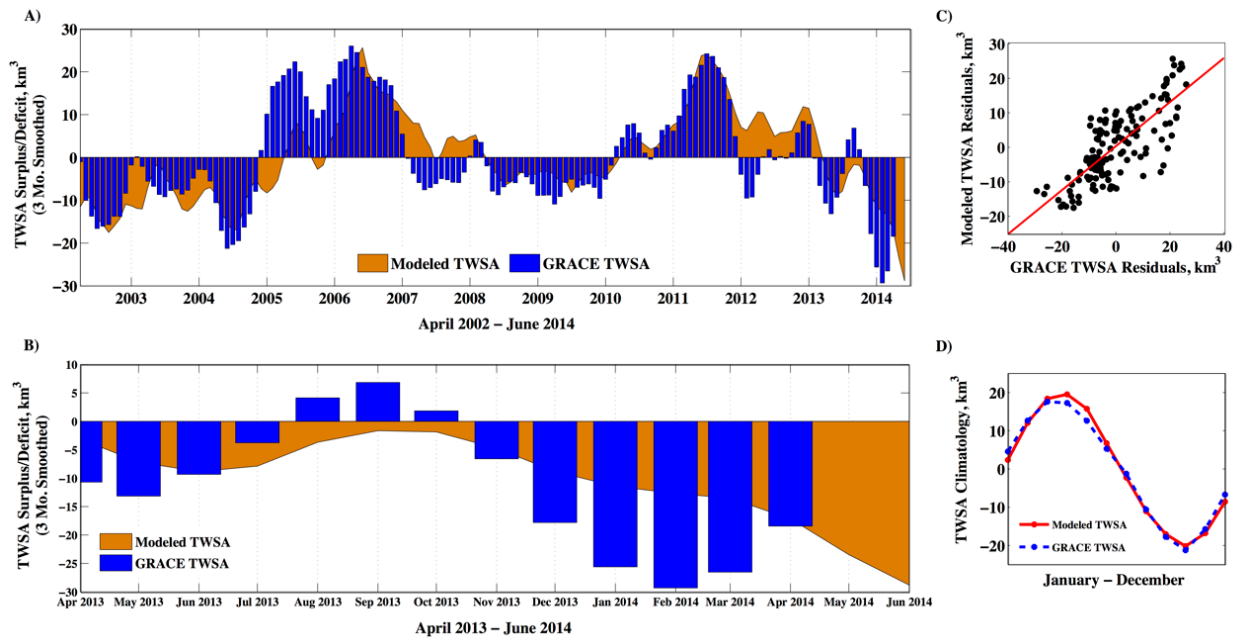
Figure 4.5. Comparison of water storage surplus and deficit from modeled storage and GRACE observations. (A) Full time series (April 2002–June 2014) GRACE (blue bars) and modeled storage (orange shading), in cubic kilometers. (B) Period from April 2013–June 2014. (C) Scatter plot of anomaly values. (D) Annual climatology of modeled (red) and observed (blue) storage. All time series have been smoothed with a 3-month low pass filter.

71
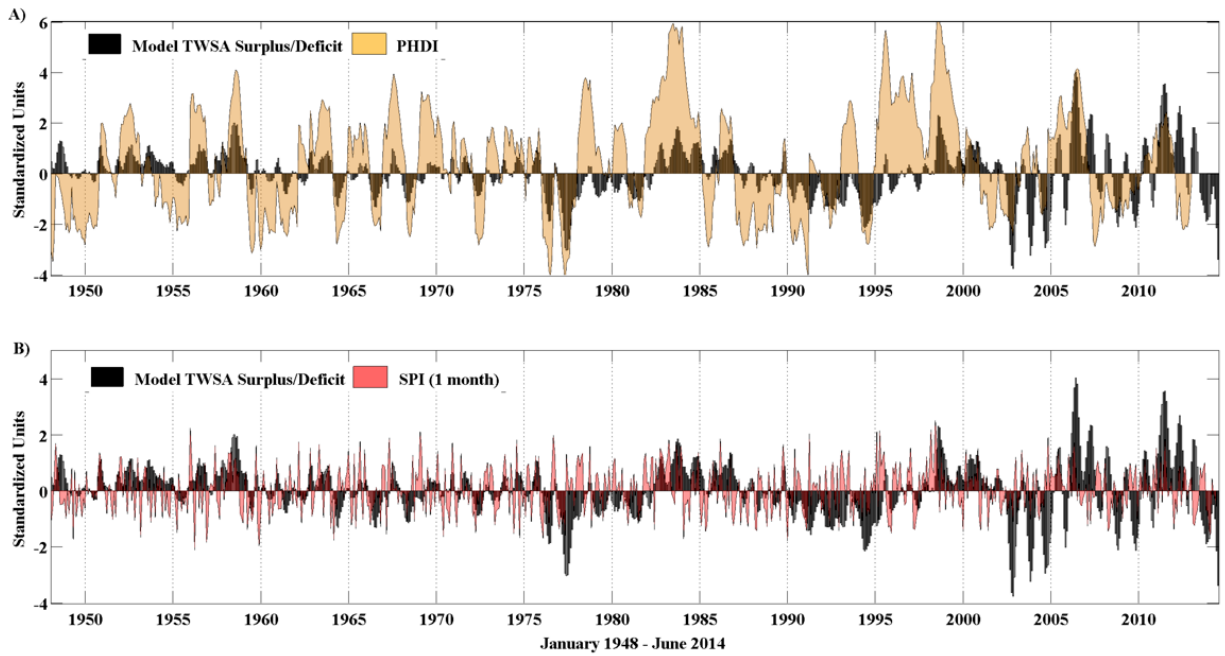
Figure 4.6. Comparison of historic PHDI, SPI (1-month), and modeled water storage extremes in the Central Valley: Model-estimated TWSA surplus and deficit (black) estimated back to January 1948 using the multi-frequency regression model with NOAA PREC/L precipitation data. *Top panel*, PHDI drought index is shown in light beige. *Bottom panel*, SPI is shown in light red. All time series are plotted in standardized units. Negative values represent storage deficits/dry months and positive represents surplus/wet months. The PHDI record extends from January 1948-December 2012. SPI extends from January 1948-May 2014.

Chapter 5

Conclusions and Future Directions

The three bodies of work presented in this dissertation illustrate that GRACE satellite data can successfully be utilized for regional scale drought analysis. The ways that I have used GRACE data in this research not only have implications for improving drought early warning lead times and drought preparation and management efforts, but they have shown the significance of the GRACE satellite mission and advocate for the development of future operations. The challenge of charactering hydrologic extremes predominantly lies in how we initially define what constitutes an "extreme", in addition to the accessibility and precision of data. When *in situ* observations are not available, we turn to remote sensing to fill in the gaps. The GRACE-based hydrologic drought metric defined drought from the viewpoint of water storage deficits. This definition of drought was utilized throughout the dissertation as a means to evaluate model-based hydrologic extremes as well as synthetic estimates of water storage deficits from a multivariate, multi-frequency regression model.

While I did successfully develop a new metric to use GRACE TWSA data to quantify the severity of hydrologic drought, GRACE's spatial and vertical resolution proved to be limiting, particularly for use in monitoring water resources in more localized capacities. We addressed these shortcomings by employing CLSM-DA TWSA outputs for extremes analysis. With CLSM-DA data, the spatial resolution TWSA improves to a quarter degree, the GRACE signal is vertically disaggregated into surface and subsurface storage components, and data latency improves to the near present month instead of a 2-5 month lag with GRACE observations. CLSM-DA was successful in identifying several flood and drought events within the United

States during the GRACE period of record with higher spatial capacity than GRACE and more accurate magnitudes than CLSM-OL.

CLSM-DA is still limited by model physics and parameters that were not able to fully achieve the amplitude of many events. Improving CLSM would require a combination of more accurate input data and improved parameterization of the model itself, to enhance simulations. With a satellite mission, like the Soil Moisture Active Passive (SMAP) [*Entekhabi et al.*, 2010], hydrologists will gain more accurate, higher resolution, and larger spatial coverage of soil moisture states across the global. These improved maps of soil moisture variations, including freeze and thaw states, will provide superior information for models to simulate subsurface storage timing and magnitude; the direct benefit being enhanced flood and drought capabilities.

During periods of prolonged drought, one of the foremost questions is: "when will the drought end?" Relating precipitation to water storage changes was a logical step towards addressing this matter; hence, the development of a multivariate, multi-frequency, linear regression model. With this model, I estimated water storage change with the current-most available precipitation data. In the Central Valley, precipitation and evapotranspiration accounted for 82% of total water storage changes.

Improvements would include augmenting the model with additional components, (*e.g.*, groundwater well and temperature data). Groundwater, which does not have a strict linear relationship with rainfall inputs [*Changnon et al.*, 1988], would add valuable information about subsurface storage changes to model. Several different 21st century climate model simulations have suggested that dry years will experience anomalously warm summer temperatures, even above and beyond the warming trend in the Southwest [*Cayan et al.,* 2010], which can exacerbate summer drought conditions. Future models may introduce lagged climate and storage

terms based on the persistence in the data. The relationships that temperature has with evaporation and transpiration [*Fitzpatrick*, 1963; *Linacre*, 1977] directly influence water storage changes, making temperature a logical variable to include in a follow-on regression model. An alternative model approach could be to build a stochastic model with distribution functions for each component of the water budget for a region and estimate the joint storage distribution.

The potential for GRACE and GRACE-associated datasets in future drought and flood research is immense. Integrated approaches, such as the regression model described in this dissertation, are important for determining future responses of water resources due to climate change [*Georgakakos et al.*, 2014]. An extension of this work would involve the use of climate model projections to estimate precipitation [*Walsh et al.*, 2014] and resulting water storage 10-50 years into the future. This information would greatly influence the planning of water infrastructure, policy, mitigation strategies, and risk assessment by providing a range of the severity hydrologic extremes with associated uncertainties.

There is not only a need to better describe the natural system response to changes in climate, there is a need to better assess the social system response when conducting water resources planning studies [*Brekke, et al.*, 2009]. *Vörösmarty et al.* [2000] emphasize the necessity of incorporating land surface and groundwater hydrology, water engineering, human system, and societal adaptations to water scarcity in climate change and variability research, though studies involving natural hydrological cycles and data about the social aspects of water use are underprovided [*Oki and Kanae*, 2006]. The uniqueness of GRACE TWSA is that it integrates changes due to human influences on the system in addition to natural changes. Further work should exploit this and push the envelope of GRACE's capabilities.

References

AghaKouchak, A. (2014), A baseline probabilistic drought forecasting framework using Standardized Soil Moisture Index: application to the 2012 United States drought, *Hydrology and Earth System Sciences Discussions*, 11(2), 1947-1966.

American Meteorological Society (2013), Drought: An Information Statement of the American Meteorological Society (Adopted by AMS Council on 19 September 2013).

Besley, D., E. Kuh, and R. Welsch (2004), *Regression diagnostics: identifying influential data and sources of multicollinearity*, Wiley, New York, NY, USA.

Beven, K. J. and M. J. Kirkby (1979), A physically-based variable contributing area model of basin hydrology, *Hydrological Sciences Journal*, 24, 43-69.

Billah, M. M. and J. L. Goodall (2011), Annual and interannual variations in terrestrial water storage during and following a period of drought in South Carolina, USA, *Journal of Hydrology*, 409(1), 472-482.

Brekke, L. D., J. E. Kiang, J. R. Olsen, R. S. Pulwarty, D. A. Raff, D. P. Turnipseed, … and K. D. White (2009), Climate change and water resources management: A federal perspective, *U.S. Geological Survey Circular*, 1331.

Breusch, T. S. and A. R. Pagan (1979), A simple test for heteroscedasticity and random coefficient variation, *Econometrica*, 47 (1979), pp. 1287-1294.

California Department of Water Resources (2014), California Data Exchange, http://cdec.water.ca.gov/misc/monthly_res.html, Accessed May 2014.

Cayan, D., K. Kunkel, C. Castro, A. Gershunov, J. Barsugli, A. Ray, J. Overpeck, M. Anderson, J. Russell, B. Rajagopalan, I. Rangwala, and P. Duffy (2013), Ch. 6: Future climate: Projected average. Assessment of Climate Change in the Southwest United States: A

Report Prepared for the National Climate Assessment, [G. Garfin, A. Jardine, R. Merideth, M. Black, and S. LeRoy (Eds.)], Island Press, 153-196.

Cayan, D. R., T. Das, D. W. Pierce, T. P. Barnett, M. Tyree, and A. Gershunov (2010), Future dryness in the southwest US and the hydrology of the early 21st century drought, *Proceedings of the National Academy of Sciences*, 107, 21271-21276, doi: 10.1073/pnas.0912391107.

Chambers, D. P., J. Wahr, M. E. Tamisiea, and R. S. Nerem (2010), Ocean mass from GRACE and glacial isostatic adjustment, *Journal of Geophysical Research*, 115, B11415, doi: 10.1029/2010JB007530.

Chang, T. J., M. L. Kavvas, and J. W. Delleur (1984), Modeling sequences of wet and dry days by binary discrete autoregressive moving average processes, *Journal of Climate and Applied Meteorology*, 23, 1367-1378.

Changnon, S. A., F. A. Huff, and C. F. Hsu (1988), Relations between precipitation and shallow groundwater in Illinois, *Journal of Climate*, 1(12), 1239-1250.

Chen, J. L., C. R. Wilson, B. D. Tapley, Z. L. Yang, and G. Y. Niu (2009), 2005 drought event in the Amazon River basin as measured by GRACE and estimated by climate models, *Journal of Geophysical Research*, 114, B05404, doi: 10.1029/2008JB006056.

Chen, M., P. Xie, J. E. Janowiak, and P. A. Arkin (2002), Global Land Precipitation: A 50-yr Monthly Analysis Based on Gauge Observations, *Journal of Hydrometeorology*, 3, 249-266.

Chung, C. H. and J. D. Salas (2000), Drought occurrence probabilities and risks of dependent hydrologic processes, *Journal of Hydrologic Engineering*, 5(3), 259-268.

Condra, G. E. (1944), Drought: Its effect and measures of control in Nebraska. *Nebraska Conservation Bull.* 25, Conservation and Survey Division, University of Nebraska, Lincoln, NE, 43 pp.

Dai, A., K. E. Trenberth, and T. Qian (2004), A global data set of Palmer Drought Severity Index for 1870-2002: Relationship with soil moisture and effects of surface warming, *Journal of Hydrometeorology*, 5, 1117-1130.

Daly, C., M. Halbleib, J. I. Smith, W. P. Gibson, M. K. Doggett, G. H. Taylor, … and P. P. Pasteris (2008), Physiographically sensitive mapping of climatological temperature and precipitation across the conterminous United States, *International Journal of Climatology*, 28(15), 2031-2064.

Dracup, J. A. (1991), Drought monitoring, *Stochastic Hydrology and Hydraulics*, 5(4), 261-266.

Dracup, J. A., K. S. Lee, and E. G. Paulson, Jr. (1980), On the definition of droughts, *Water Resources Research*, *16*(2), 297-302.

Durbin, J. and G. S. Watson (1950), Testing for Serial Correlation in Least Squares Regression, I, *Biometrika*, 37 (3-4): 409-428. doi: 10.1093/biomet/37.3-4.409.

Ek, M. B., K. E. Mitchell, Y. Lin, E. Rogers, P. Grunmann, V. Koren, G. Gayno, and J. D. Tarpley (2003), Implementation of Noah land surface model advances in the National Centers for Environmental Prediction operational mesoscale Eta model, *Journal of Geophysical Research*, 108(D22), 8851, doi:10.1029/2002JD003296.

Elathir, E. A. B. and P. J.-F. Yeh (1999), On the asymmetric response of aquifer water level to floods and droughts in Illinois, *Water Resources Research*, 35(4), 1199-1217.

EM-DAT: The OFDA/CRED International Disaster Database (2013; 2014), Universite

    catholique de Louvain, Brussels, Belgium, http://www.emdat.be/, Accessed January 2013

    and May 2014.

Entekhabi, D., E. G. Njoku, P. E. O'Neill, K. H. Kellogg, W. T. Crow, W. N. Edelstein, … and J.

    Van Zyl (2010), The soil moisture active passive (SMAP) mission, *Proceedings of the IEEE*,

    98(5), 704-716.

Famiglietti, J. S. and E. F. Wood (1994a), Multiscale modeling of spatially variable water and

    energy balance processes, *Water Resources Research*, 30, 3061-3078.

Famiglietti, J. S. and E. F. Wood (1994b), Application of multiscale water and energy balance

    models on a tallgrass prairie, *Water Resources Research*, 30, 3079-3093.

Famiglietti, J. S., and M. Rodell, 2013, Water in the Balance, invited Perspective, *Science*, 340,

    1300, doi: 10.1126/science.1236460.

Famiglietti, J. S., M. Lo, S. L. Ho, J. Bethune, K. J. Anderson, T. H. Syed, S. C. Swenson, C. R.

    de Linage, and M. Rodell (2011), Satellites measure recent rates of groundwater

    depletion in California's Central Valley, *Geophysical Research Letters*, 38, L03403,

    doi:10.1029/2010GL046442.

Faunt, C.C. (Ed.) (2009), Groundwater Availability of the Central Valley Aquifer, *California:*

    U.S. Geological Survey Professional Paper, 1766, 225 p.

Fitzpatrick, E. A. (1963), Estimates of pan evaporation from mean maximum temperature and

    vapor pressure, *Journal of Applied Meteorology*, 2(6), 780-792.

Forman, B. A. and R. H. Reichle (2013), The spatial scale of model errors and assimilated

    retrievals in a terrestrial water storage assimilation system, *Water Resources Research*,

    49(11), 7457-7468.

Forootan, E., R. Rietbroek, J. Kusche, M. A. Sharifi, J. L. Awange, M. Schmidt, … and J. S. Famiglietti (2014), Separation of large scale water storage patterns over Iran using GRACE, altimetry and hydrological data, *Remote Sensing of Environment*, 140, 580-595.

Frappart, F., F. Papa, J. S. da Silva, G. Ramillien, C. Prigent, F. Seyler, and S. Calmant (2012), Surface freshwater storage and dynamics in the Amazon basin during the 2005 exceptional drought, *Environmental Research Letters*, *7* (4), 044010.

Frappart, F., F. Papa, J. S. Famiglietti, C. Prigent, W. B. Rossow, and F. Seyler (2008), Interannual variations of river water storage from a multiple satellite approach: A case study for the Rio Negro River basin, *Journal of Geophysical Research*, 113, D21104, doi:10.1029/2007JD009438.

Gascoin, S., A. Ducharne, P. Ribstein, M. Carli, and F. Habets (2009), Adaptation of a catchment-based land surface model to the hydrogeological setting of the Somme River basin (France), *Journal of Hydrology*, 368, 105(116), doi:10.1016/j.jhydrol.2009.01.039.

Georgakakos, A., P. Fleming, M. Dettinger, C. Peters-Lidard, T. C. Richmond, K. Reckhow, K. White, and D. Yates (2014), Ch. 3: Water Resources. Climate Change Impacts in the United States: The Third National Climate Assessment, [J. M. Melillo, T. C. Richmond, and G. W. Yohe (Eds.)], U.S. Global Change Research Program, 69-112, doi:10.7930/ J0G44N6T.

Gleick, P., H. Cooley, K. Poole, and E. Osann (2014), *Issue Brief: The Untapped Potential of California's Water Supply: Efficiency, Reuse, and Stormwater*, Pacific Institute and Natural Resources Defense Council, IB:14-05-C.

Guttman, N. B. (1999), Accepting the Standandardized Precipitation Index: a calculation algorithm. Journal of American Water Resources Association, 35(2), 311-322.

Hanak, E. and J. R. Lund (2012), Adapting California's water management to climate change, *Climatic Change*, 111(1), 17-44.

Hasegawa, T., Y. Fukuda, K. Yamamoto, and T. Nakaegawa (2008), The 2006 Australian drought detected by GRACE, Headwaters to the ocean, Taylor & Francis Group, London, 363-367.

Havens, A. V. (1954), Drought and agriculture, *Weatherwise*, *7*(3), 51-68.

Hayes M. J. (2006), What Is Drought? Drought Indices, Lincoln, NE: National Drought Mitigation Center.

Heim, R. R., Jr. (2002), A review of twentieth-century drought indices used in the United States. *Bulletin of the American Meteorological Society*, *83*(8), 1149-1165.

Houborg, R., M. Rodell, B. Li, R. Reichle, and B. Zaitchik (2012), Drought indicators based on model assimilated GRACE terrestrial water storage observations, *Water Resources Research*, 48, W07525, doi:10.1029/2011WR011291.

Howitt, R., J. Medellin-Azuara, and J. Lund (2014), Preliminary 2014 Drought Economic Impact Estimates in Central Valley Agriculture, 1-6 pp.

Intergovernmental Panel on Climate Change, IPCC (2013), Summary for Policymakers. In: *Climate Change 2013: The Physical Science Basis. Contribution of Working Group I to the Fifth Assessment Report of the Intergovernmental Panel on Climate Change* [Stocker, T. F., D. Qin, G. -K. Plattner, M. Tignor, S. K. Allen, J. Boschung, A. Nauels, Y. Xia, V. Bex and P. M. Midgley (eds.)], Cambridge University Press, Cambridge, United Kingdom and New York, NY, USA.

IPCC (2007), *Climate Change 2007: The Physical Science Basis*, Contribution of Working Group I to the Fourth Assessment Report of the Intergovernmental Panel on Climate

Change, [Solomon, S., D. Qin, M. Manning, Z. Chen, M. Marquis, K. B. Averyt, M. Tignor and H. L. Miller (eds.)], Cambridge University Press, Cambridge.

Jacobs, P. A. and P. A. W. Lewis (1978), Discrete time series generated by mixtures I: correlational and runs properties, *Journal of the Royal Statistical Society*, Series B, 40, 94-105.

Jongen, M., J. S. Pereira, L. M. I. Aires, and C. A. Pio (2011), The effects of drought and timing of precipitation on the inter-annual variation in ecosystem-atmosphere exchange in a Mediterranean grassland, *Agricultural and Forest Meteorology*, 151(5), 595-606.

Joodaki, G., J. Wahr, and S. Swenson (2014), Estimating the human contribution to groundwater depletion in the Middle East, from GRACE data, land surface models, and well observations, *Water Resources Research*, 50, 2679–2692, doi:10.1002/ 2013WR014633.

Kallis, G. (2008), Droughts, *Annual Review of Environment and Resources*, *33*(1), 85.

Karl, T. and R. W. Knight (1985), Atlas of monthly Palmer hydrological drought indices (1931-1983) for the contiguous United States, National Climatic Data Center.

Karl, T.R., J. M. Melillo, and T. C. Peterson (eds.) (2009), Global Climate Change Impacts in the United States, United States Global Change Research Program, Cambridge University Press, New York, NY, USA.

Katz, R. W., M. B. Parlange, and P. Naveau (2002), Statistics of extremes in hydrology, *Advances in Water Resources*, 25(8), 1287-1304.

Keyantash, J. and J. A. Dracup (2002), The quantification of drought: an evaluation of drought indices, *Bulletin of the American Meteorological Society*, *83*(8), 1167-1180.

Koster, R. D., M. J. Suarez, A. Ducharne, M. Stieglitz, and P. Kumar (2000), A catchment-based approach to modeling land surface processes in a general circulation model 1. Model

structure, *Journal of Geophysical Research: Atmospheres (1984–2012)*, 105 (24) 809-822.

Kunkel, K. E., L. E. Stevens, S. E. Stevens, L. Sun, E. Janssen, D. Wuebbles, K. T. Redmond, and J. G. Dobson (2013a), Regional Climate Trends and Scenarios for the U.S. National Climate Assessment: Part 5. Climate of the Southwest U.S., *NOAA Technical Report*, NESDIS, National Oceanic and Atmospheric Administration, National Environmental Satellite, Data, and Information Service, Washington, D.C., 142-5, 87 pp.

Kunkel, K. E., L. E. Stevens, S. E. Stevens, L. Sun, E. Janssen, D. Wuebbles, and J. G. Dobson (2013b), Regional Climate Trends and Scenarios for the U.S. National Climate Assessment: Part 9. Climate of the Contiguous United States, *NOAA Technical Report*, NESDIS, National Oceanic and Atmospheric Administration, National Environmental Satellite, Data, and Information Service, Washington, D.C., 142-9. 85 pp.

Landerer, F. W., and S. C. Swenson (2012), Accuracy of scaled GRACE terrestrial water storage estimates, *Water Resources Research*, 48, W04531, doi: 10.1029/2011WR011453.

Leblanc, M. J., P. Tregoning, G. Ramillien, S. O. Tweed, and A. Fakes (2009), Basin-scale, integrated observations of the early 21st century multiyear drought in southeast Australia, *Water Resources Research*, *45*, W04408, doi: 10.1029/2008WR007333.

Li, B., M. Rodell, B. Zaitchick, R. Reichle, R. Koster and T. van Dam (2012), Assimilation of GRACE terrestrial water storage into a land surface model: Evaluation and potential value for drought monitoring in western and central Europe, *Journal of Hydrology*. doi:http://dx.doi.org/10.1016/j.jhydrol.2012.04.035.

Linacre, E. T. (1977), A simple formula for estimating evaporation rates in various climates using temperature data alone, *Agricultural Meteorology*, 18(6), 409-424.

Linsley, R. K., Jr., M. A. Kohler, J. C. H. Paulhus (1975), <u>Hydrology for Engineers</u>, McGraw-Hill, New York.

Long, D., B. R. Scanlon, L. Longuevergne, A. -Y. Sun, D. N. Fernando, and H. Save (2013), GRACE satellites monitor large depletion in water storage in response to the 2011 drought in Texas, *Geophysical Research Letters*, 40, 3395-3401, doi:10.1002/grl.50655.

Lynch-Stieglitz, M. (1994), The development and validation of a simple snow model for the GISS GCM, *Journal of Climate*, 7, 1842-1855.

McKee, T. B., N. J. Doesken, and J. Kleist (1993), The relationship of drought frequency and duration to time scales, *In Proceedings of the 8th Conference on Applied Climatology* (Vol. 17, No. 22, pp. 179-183), Boston, MA: American Meteorological Society.

Meehl, G. A. (1987), The annual cycle and interannual variability in the tropical pacific and Indian ocean regions, *Monthly Weather Review*, 115, 27–50. doi: http://dx.doi.org/10.1175/1520-0493(1987)115<0027:TACAIV>2.0.CO;2

Mishra, A. K., V. P. Singh, and V. R. Desai (2009), Drought characterization: a probabilistic approach, *Stochastic Environmental Research and Risk Assessment*, 23(1), 41-55.

Mu, Q., M. Zhao, J. S. Kimball, N. G. McDowell, and S. W. Running (2013), A Remotely Sensed Global Terrestrial Drought Severity Index, *Bulletin of the American Meteorological Society*, *94*, 83-98.

Njoku, E. G. (2004), AMSR-E/Aqua Daily L3 Surface Soil Moisture, Interpretive Parameters, & QC EASE-Grids, Version 2, [AMSR_E_L3_DailyLand], Boulder, Colorado USA: NASA DAAC at the National Snow and Ice Data Center.

Njoku, E. G., T. J. Jackson, V. Lakshmi, T. K. Chan, and S. V. Nghiem (2003), Soil moisture retrieval from AMSR-E, *Geoscience and Remote Sensing*, IEEE Transactions on, 41(2), 215-229.

Oki, T. and S. Kanae (2006), Global hydrological cycles and world water resources, *Science*, 313(5790), 1068-1072.

Oleson, K. W., G. Y. Niu, Z. L. Yang, D. M. Lawrence, P. E. Thornton, P. J. Lawrence, … and T. Qian (2008), Improvements to the Community Land Model and their impact on the hydrological cycle, *Journal of Geophysical Research: Biogeosciences* (2005-2012), 113(G1).

Overgaard, J., D. Rosbjerg, M. B. Butts (2006), Land-surface modelling in hydrological perspective – a review, *Biogeosciences*, 3:229-241.

Palmer, W. C (1965), Meteorological Drought, *Research Paper No. 45*, 58 pp., Department of Commerce, Washington, D.C.

Panu, U. S. and T. C. Sharma (2002), Challenges in drought research: some perspectives and future directions, *Hydrological Sciences Journal*, *47*(S1), S19-S30.

PRISM Climate Group, Oregon State University, http://prism.oregonstate.edu. Accessed May, 2014.

Ramillien, G., J. S. Famiglietti, and J. Wahr (2008), Detection of Continental Hydrology and Glaciology Signals from GRACE: A Review, *Surveys in Geophysics*, 29, 361-374, doi: 10.1007/s10712-008-9048-9.

Reager, J. T., and J. S. Famiglietti (2009), Global terrestrial water storage capacity and flood potential using GRACE, *Geophysical Research Letters*, 36, L23402, doi: 10.1029/2009GL040826.

Reichle, R. H. and R. D. Koster (2005), Global assimilation of satellite surface soil moisture retrievals into the NASA Catchment land surface model, *Geophysical Research Letters*, 32, L02404, doi: 10.1029/2004GL021700.

Reichle, R. H., D. B. McLaughlin, and D. Entekhabi (2002a), Hydrologic data assimilation with the ensemble Kalman filter, *Monthly Weather Review*, 130, 103-114.

Reichle, R. H., J. P. Walker, R. D. Koster, and P. R. Houser (2002b), Extended versus ensemble Kalman filtering for land data assimilation, *Journal of Hydrometeorology*, 3, 728-740.

Reichle, R. H., M. G. Bosilovich, W. T. Crow, R. D. Koster, S. V. Kumar, S. P. Mahanama, and B. F. Zaitchik (2009), *Recent advances in land data assimilation at the NASA Global Modeling and Assimilation Office*, Data Assimilation for Atmospheric, Oceanic and Hydrologic Applications, Springer Berlin Heidelberg, pp. 407-428.

Reichle, R. H., R. D. Koster, P. Liu, S. P. P. Mahanama, E. G. Njoku, and M. Owe (2007), Comparison and assimilation of global soil moisture retrievals from the Advanced Microwave Scanning Radiometer for the Earth Observing System (AMSR-E) and the Scanning Multichannel Microwave Radiometer (SMMR), *Journal of Geophysical Research*, 112, D09108, doi:10.1029/2006JD008033.

Rodell, M. and J. S. Famiglietti (1999), Detectability of variations in continental water storage from satellite observations of the time dependent gravity field, *Water Resources Research*, 35(9), 2705-2723.

Rodell, M. and J. S. Famiglietti (2001), An analysis of terrestrial water storage variations in Illinois with implications for the Gravity Recovery and Climate Experiment (GRACE), *Water Resources Research*, 37(5), 1327-1339.

Rodell, M., B. Zaitchik, and R. Reichle (2010), Remote Sensing of Terrestrial Water Storage and Application to Drought Monitoring, Retrieved March 2014 from www.drought.gov.

Rodell, M., I. Velicogna, and J. S. Famiglietti (2009), Satellite-based estimates of groundwater depletion in India, *Nature*, 460(7258), 999-1002.

Rodell, M., J. Chen, H. Kato, J. S. Famiglietti, J. Nigro, and C. R. Wilson (2007), Estimating groundwater storage changes in the Mississippi River basin (USA) using GRACE, *Hydrogeology Journal*, 15(1), 159-166.

Rodell, M., P. R. Houser, U. E. A. Jambor, J. Gottschalck, K. Mitchell, C. J. Meng, … and D. Toll (2004), The global land data assimilation system, *Bulletin of the American Meteorological Society*, 85(3), 381-394.

Schmidt, R., F. Flechtner, U. Meyer, K-H. Neumayer, C. Dahle, R. König, and J. Kusche (2008), Hydrological signals observed by the GRACE satellites, *Surveys in Geophysics*, (29), 4, 319-334.

Seo, K.-W., C. R. Wilson, J. S. Famiglietti, J. L. Chen, and M. Rodell (2006), Terrestrial water mass load changes from Gravity Recovery and Climate Experiment (GRACE), *Water Resources Research*, 42 (5), W05417, doi: 10.1029/2005WR004255.

Sheffield, J., E. F. Wood, and M. L. Roderick (2012), Little change in global drought over the past 60 years, *Nature*, 491(7424), 435-438.

Sheffield, J., G. Goteti, and E. F. Wood (2006), Development of a 50-year high-resolution global dataset of meteorological forcings for land surface modeling, *Journal of Climate*, 19(13), 3088-3111.

Sophocleous, M. (2002), Interactions between groundwater and surface water: the state of the science, *Hydrogeology Journal*, 10(1), 52-67.

Stedinger, J. R., R. M. Vogel, and E. Foufoula-Georgiou (1993), Frequency analysis of extreme events, *Handbook of Hydrology*, Chapter 18, [D. R. Maidment (ed.)], McGraw-Hill, New York, 18.1-18.66.

Stieglitz, M., D. Rind, J. Famiglietti, and C. Rosenzweig (1997), An Efficient Approach to Modeling the Topographic Control of Surface Hydrology for Regional and Global Climate Modeling, *Journal of Climate*, 10, 118-137. doi: http://dx.doi.org/10.1175/1520-0442(1997)010<0118:AEATMT>2.0.CO;2.

Sun, F. and J. Y. Yu (2009), A 10-15-yr modulation cycle of ENSO intensity, *Journal of Climate*, 22(7), 1718-1735.

Svoboda, M., D. LeComte, M. Hayes, R. Heim, K. Gleason, J. Angel, … and S. Stephens (2002), The drought monitor, *Bulletin of the American Meteorological Society*, 83(8), 1181-1190.

Swenson, S. C. and J. Wahr (2002), Methods for inferring regional surface mass anomalies from GRACE measurements of time-variable gravity, *Journal of Geophysical Research*, 107(B9), 2193, doi: 10.1029/2001JB000576.

Swenson, S. C. and J. Wahr (2006), Post-processing removal of correlated errors in GRACE data, *Geophysical Research Letters*, 33, L08402, doi: 10.1029/2005GL025285.

Syed, T. H., J. S. Famiglietti, V. Zlotnicki, and M. Rodell (2007), Contemporary estimates of Pan-Arctic freshwater discharge from GRACE and reanalysis, *Geophysical Research Letters*, 34, L19404, doi: 10.1029/2007GL031254.

Tallaksen, L. M. and H. A. Van Lanen (Eds.) (2004), *Hydrological Drought: Processes and Estimation Methods for Streamflow and Groundwater*, Vol. 48, Elsevier.

Tallaksen, L. M., H. Madsen, and B. Clausen (1997), On the definition and modelling of streamflow drought duration and deficit volume, *Hydrological Sciences Journal*, 42:1, 15-33.

Tapley, Byron D., S. Bettadpur, J. C. Ries, P. F. Thompson, and M. M. Watkins (2004), GRACE Measurements of Mass Variability in the Earth System. *Science*, 305 (5683), 503, doi: 10.1126/science.1099192.

Thomas, A. C., J. T. Reager, J. S. Famiglietti, M. and Rodell (2014), A GRACE-based water storage deficit approach for hydrological drought characterization, *Geophysical Research Letters*, 41(5), 1537-1545.

Tiwari, V. M., J. Wahr, and S. C. Swenson (2009), Dwindling groundwater resources in northern India, from satellite gravity observations, *Geophysical Research Letters*, 36, L18401, doi: 10.1029/2009GL039401.

U.S. Drought Monitor (2013, 2014), University of Nebraska-Lincoln, National Drought Mitigation Center (NDMC), the U.S. Department of Agriculture (USDA), and the National Oceanic and Atmospheric Administration (NOAA). http://droughtmonitor.unl.edu/archive.html. Accessed August 2013.

Velicogna, I. (2009). Increasing rates of ice mass loss from the Greenland and Antarctic ice sheets revealed by GRACE. *Geophysical Research Letters*, 36, doi: 10.1029/2009gl040222.

Velicogna, I. and J. Wahr (2006), Measurements of time-variable gravity show mass loss in Antarctica, *Science*, 311, 1754, doi: 10.1126/science.1123785.

Vicente-Serrano, S. M. and J. I. López-Moreno (2005), Hydrological response to different time scales of climatological drought: an evaluation of the Standardized Precipitation Index in

a mountainous Mediterranean basin, *Hydrology and Earth System Sciences Discussions*
9.5: 523-533.

Vörösmarty, C. J., P. Green, J. Salisbury, and R. B. Lammers (2000), Global water resources:
vulnerability from climate change and population growth, *Science*, 289(5477), 284-288.

Voss, K. A., J. S. Famiglietti, M. Lo, C. de Linage, M. Rodell, and S. C. Swenson (2013),
Groundwater depletion in the Middle East from GRACE with implications for
transboundary water management in the Tigris-Euphrates-Western Iran region, *Water Resource Research*, 49, 904-914, doi:10.1002/wrcr.20078.

Wahr, J., M. Molenaar, and F. Bryan (1998), Time-variability of the Earth's gravity field:
Hydrological and oceanic effects and their possible detection using GRACE, *Journal of Geophysical Research*, 103, 30,205–30,230.

Wahr, J., S. Swenson, and I. Velicogna (2006), Accuracy of GRACE mass estimates,
Geophysical Research Letters, 33, L06401, doi : 10.1029/2005GL025305.

Wahr, J., S. C. Swenson, V. Zlotnicki, I. Velicogna (2004), Time-Variable Gravity from
GRACE: First Results, *Geophysical Research Letters*, 31, doi: 10.1029/2004GL019779.

Wallace, J. M., E. M. Rasmusson, T. P. Mitchell, V. E. Kousky, E. S. Sarachik, and H. V. Storch
(1998), On the structure and evolution of ENSO-related climate variability in the tropical
Pacific: Lessons from TOGA, *Journal of Geophysical Research: Oceans* (1978-2012),
103(C7), 14241-14259.

Walsh, J., D. Wuebbles, K. Hayhoe, J. Kossin, K. Kunkel, G. Stephens, P. Thorne, R. Vose, M.
Wehner, J. Willis, D. Anderson, S. Doney, R. Feely, P. Hennon, V. Kharin, T. Knutson, F.
Landerer, T. Lenton, J. Kennedy, and R. Somerville (2014), Ch. 2: Our Changing Climate.
Climate Change Impacts in the United States: The Third National Climate Assessment, [J. M.

Melillo, T. C. Richmond, and G. W. Yohe (Eds.)], U.S. Global Change Research Program, 19-67, doi:10.7930/J0KW5CXT.

Wilhite, D. A. and M. H. Glantz (1985), Understanding: the drought phenomenon: the role of definitions, *Water International*, *10*(3), 111-120.

Wilhite, D. A., M. D. Svoboda, and M. J. Haye (2007), Understanding the complex impacts of drought: a key to enhancing drought mitigation and preparedness, *Water Resources Management*, *21*(5), 763-774.

Willmott, C. J. (1981), On the validation of models, *Physical Geography*, 2(2), 184-194.

Wood, E. F., J. K. Roundy, T. J. Troy, L. P. H. Van Beek, M. F. Bierkens, E. Blyth, ... and P. Whitehead (2011), Hyperresolution global land surface modeling: Meeting a grand challenge for monitoring Earth's terrestrial water, *Water Resources Research*, 47(5).

Yang, Z. L., G. Y. Niu, K. E. Mitchell, F. Chen, M. B. Ek, M. Barlage, ... and Y. Xia (2011), The community Noah land surface model with multiparameterization options (Noah-MP): 2, Evaluation over global river basins, *Journal of Geophysical Research: Atmospheres (1984-2012)*, 116(D12).

Yeh, P., S. C. Swenson, J. S. Famiglietti, and M. Rodell (2006), Remote sensing of groundwater storage changes in Illinois using the Gravity Recovery and Climate Experiment (GRACE), *Water Resources Research*, 42, W12203, doi: 10.1029/2006WR005374.

Yevjevich, V. (1967), <u>An objective approach to definitions and investigations of continental hydrologic droughts</u>, Fort Collins: Colorado State University.

Yirdaw, S. Z., K. R. Snelgrove, C. O. Agboma (2008), GRACE satellite observations of terrestrial moisture changes for drought characterization in the Canadian Prairie, *Journal of Hydrology*, 56, 84-92.

Zaitchik, B. F., M. Rodell, and R. H. Reichle (2008), Assimilation of GRACE terrestrial water storage data into a land surface model: results for the Mississippi River Basin, *Journal of Hydrometeorology*, 9 (3), 535-548, doi: 10.1175/2007JHM951.

Zaitchik, B. F., M. Rodell, S. Kumar, R. H. Reichle, J. D. Bolten, and K. Bergaoui (2013), Recent Advances in the GRACE Data Assimilation System, In AGU Fall Meeting Abstracts, Vol. 1, p. 02.

Zhang, Y., J. M. Wallace, and N. Iwasaka (1996), Is Climate Variability over the North Pacific a Linear Response to ENSO?, *Journal of Climate*, 9, 1468-1478.

Zhao, W. and Khalil, M. A. K. (1993), The relationship between precipitation and temperature over the contiguous United States, *Journal of Climate*, 6(6), 1232-1236.